INVESTIGATION OF NEUROVASCULAR COUPLING BY SYNCHRONOUS EEG AND fNIRS MEASUREMENTS DURING STEADY-STATE VISUAL STIMULI

by

Müge Özker

B.S. in Electrical and Electronics Engineering, Koç University, 2007

M.S. in Biomedical Engineering, Boğaziçi University, 2009

Submitted to the Institute of Biomedical Engineering

in partial fulfillment of the requirements

for the degree of

Master of Science

in

Biomedical Engineering

Boğaziçi University

June 2009

ACKNOWLEDGMENTS

First of all, I would like to thank my supervisor Associate Prof. Dr. Akın for his guidance and support throughout this research. His motivation and encouragement inspired me to better focus on my studies and to work harder.

I would like to express my gratitude to Prof. Dr. Ademoglu and to Prof. Dr. Demiralp for being a constant source of guidance and insight for my research and to the Physiology Department of Istanbul University Medical Faculty for helping me to perform my experiments in their lab.

I am indebted to Deniz Nevşehirli for his crucial help in designing the fNIRS probe and I am very grateful to my dear friends for their participation in my long and exhausting experiments with great patience and devotion.

Lastly, I want to express my gratitude to my family by dedicating this work to them. They have always backed me up and supported me with an enormous confidence, altruism and love.

ABSTRACT

INVESTIGATION OF NEUROVASCULAR COUPLING BY SYNCHRONOUS EEG AND fNIRS MEASUREMENTS DURING STEADY-STATE VISUAL STIMULI

In this thesis, the steady state human visual evoked potentials that are generated in response to visual stimulation and its corresponding hemodynamic response are investigated via electroencephalography (EEG) and functional near infrared spectroscopy (fNIRS).

The ssVEPs are investigated for the frontal and the occipital cortex and the corresponding HBO2 changes are investigated for the frontal cortex. The left and the right hemispheres are compared as well as the frontal and the occipital cortecies in terms of electrical activity and the hemodynamic response. The stimulus locked ssVEPs are time averaged in order to increase the signal to noise ratio and the power of the resulting averaged signals are calculated. On the other hand the mean values of the band passed filtered HBO2 signal for the stimulation intervals are calculated. The responses obtained from the frontal electrodes and fNIRS channels are averaged as well as the responses obtained from the occipital electrodes in order to see the overall electrophysiological and hemodynamic responses of the frontal and the occipital regions since the lateral response differences turned out to be statistically insignificant. The overall average calculated between the 13 subjects revealed that the ssVEP power observed for the frontal electrodes peak at the upper alpha band (10-13 Hz), and the ssVEP power peaks at 9 Hz frequency for the occipital electrodes, whereas the maximum hemodynamic response is observed at 24 Hz stimulation frequency.

The correlation of the ssVEP and the hemodynamic responses obtained from the frontal cortex are analyzed. At 9, 12 and 20 Hz stimulation frequencies, the linear relationship between the ssVEP and the hemodynamic responses is determined to be positive and moderate. At 28 and 30 Hz stimulation frequencies a negative, moderate correlation is found between the ssVEP and the hemodynamic responses. Since, the

maximal frontal ssVEP power and a moderate correlation between the ssVEP and the hemodynamic responses are both observed during 12 Hz visual stimulation, 12 Hz is assumed to elicit a strong neurovascular coupling in the frontal cortex.

Keywords: fNIRS, EEG, ssVEP, hemodynamic response, frontal cortex, occipital cortex.

ÖZET

NÖROVASKÜLER KUPLAJIN DURAĞAN HAL GÖRSEL UYARAN ESNASINDA SENKRON EEG VE İYKAS ÖLÇÜMLERI İLE İNCELENMESİ

Bu tezde, farklı frekans değerlerindeki görsel uyaranlara karşılık olarak ortaya çıkan durağan hal görsel uyarılmış potansiyeller ve bunlara bağlı olarak otaya çıkan hemodinamik yanıtlar elektroensefalografi (EEG) ve işlevsel yakın kızılaltı spektroskopi (iYKAS) yöntemleri ile incelenmiştir.

Durağan hal görsel uyarılmış potansiyeller frontal ve oksipital korteksler için, ilgili HBO2 yanıtı ise frontal korteks için incelenmiştir. Hem sol ve sağ hemisferlerin, hem de frontal ve oksipital kortekslerin elektriksel aktiviteleri ve hemodinamik yanıtları birbirleriyle kıyaslanmıştır. Uyarana kilitli durağan hal görsel uyarılmış potansiyellerin, sinyal-gürültü oranını arttırmak için zamansal ortalamaları bulunmuş ve ortalaması alınmış sinyallerin kuvvetleri hesaplanmıştır. Diğer bir yandan uyaran aralıklarına denk gelen HBO2 sinyalleri bant geçiren süzgeçten geçirildikten sonra ortalama değerleri hesaplanmıştır. Lateral yanıt farkları istatistiksel olarak anlamlı olmadığı için, frontal ve oksipital bölgelerden oluşan yaygın elektrofizyolojik ve hemodinamik yanıtların incelenmesi amacıyla frontal elektrotlardan, oksipital elektrotlardan ve İYKAS kanallarından elde edilen yanıtların ortalamaları hesaplanmıştır. Elde edilen 13 deneğe ait yanıtların ortalaması alındığında, frontal ve oksipital elektrotlarda gözlemlenen durağan hal görsel uyarılmış potansiyel kuvvetinin sırasıyla üst alfa bandında (10-13 Hz) ve 9 Hz de en yüksek değerlerine ulaştığı, frontal bölgede meydana gelen en yüksek hemodinamik yanıtın ise 24 Hz lik uyarana karşılık oluştuğu belirlenmiştir.

Frontal korteksten elde edilen durağan hal görsel uyarılmış potansiyellerin ve hemodinamik yanıtların ilintileri analiz edilmiştir. 9, 12 ve 20 Hz uyaran frekanslarında, durağan hal görsel uyarılmış potansiyeller ile hemodinamik yanıtların arasındaki doğrusal ilintinin, pozitif ve orta dereceli olduğu saptanmıştır. 28 ve 30 Hz uyaran frekanslarında ise bu ilintinin negatif ve orta dereceli olduğu bulunmuştur. Hem en yüksek frontal du-

rağan hal görsel uyarılmış potansiyel kuvvetinin, hem de durağan hal görsel uyarılmış potansiyel ve hemodinamik yanıt arasındaki orta dereceli ilintinin 12 Hz lik görsel uyarana karşılık elde edilmesi, bu uyaran frekansının frontal kortekste kuvvetli bir nörovasküler kuplaja neden olduğunu düşündürmektedir.

Anahtar Sözcükler: İYKAS, EEG, Durağan Hal Görsel Uyarılmış Potansiyel, Hemodinamik Yanıt, Frontal Korteks, Oksipital Korteks.

TABLE OF CONTENTS

LIST OF FIGURES

LIST OF SYMBOLS

A	Absorbance of the compound
$B(\lambda)$	Differential path length factor
C	Concentration of the compound ($molL^{-1}$)
$\epsilon(\lambda)$	Molar absorption coefficient as a function of wavelength($Lmol^{-1}cm^{-1}$)
$ep(t)$	Single evoked response
G	Signal loss due to light scattering
I	Transmitted light intensity
I_0	Incident light intensity
L	Optical path length through the medium (cm)
N	Number of trials
R	Amount of noise on a single trial
$s(t)$	Impulse train
$ssep(t)$	Steady state evoked response
$S_{ssep}(jw)$	Frequency domain representation of the steady state evoked response
$S_{ep}(jw)$	Frequency domain representation of the single evoked response
$S_s(jw)$	Frequency domain representation of the impulse train
t_0	Start time of the measurement
t_1	End time of the measurement

LIST OF ABBREVIATIONS

ATP	Adenosine TriPhosphate
BOLD	Blood Oxygen Level Dependent
BV	Blood Volume
CBF	Cerebral Blood Flow
rCBF	Regional Cerebral Blood Flow
CMRO2	Cerebral Metabolic Rate of Oxygen
CNS	Central Nervous System
CO2	Carbon Dioxide
ECD	Equivalent Current Dipole
EEG	Electroencephalography
EP	Evoked Potential
ERP	Event Related Potential
fMRI	Functional Magnetic Resonance Imaging
fNIRS	Functional Near Infrared Spectroscopy
GLM	General linear models
HB	Deoxyhemoglobin
HBO2	Oxyhemoglobin
ICA	Independent Component Analysis
tHB	Total Hemoglobin
NIRS	Near Infrared Spectroscopy
NVC	Neurovascular Coupling
Oxy	Oxygenation
PET	Positron Emission Tomography
PNS	Peripheral Nervous System
ssEP	Steady State Evoked Potential
ssVEP	Steady State Visual Evoked Potential
ssVER	Steady State Visual Evoked Response
S/N	Signal-to-Noise ratio

VEP	Visaul Evoked Potential

1. INTRODUCTION

1.1 Motivation

The electrical activity of the brain in response to a presented stimulus has been studied for decades and has provided insight into the brain mechanisms. Auditory, somatosensory and visual evoked potentials can be used as the indicators of various neurological diseases and sensory disorders.

The stimulus dependent response of the brain is named event related potential (ERP) and it is distinct from the ongoing background EEG activity. ERPs can be generated in response to a sensory stimulus or to cognitive tasks. The electrical potentials generated by the brain in response to a sensory stimulus are named evoked potentials (EPs). Sensory stimulus can be in the form of auditory stimulus (e.g. presentation of a sound), somatic stimulus (e.g. touch, vibration) or visual stimulus (e.g. flashing lights, alternating checkerboards).

Response of the brain to a single sensory stimulus is overlapped with the responses to other stimuli when repetitive sensory stimuli is applied and the result from the superposition of the transient responses is called the steady state evoked potential (ssEP). Steady state evoked potential includes the same fundamental frequency as the stimulation as well as the higher harmonics. The phases and the amplitudes of the frequency components of the response remain constant over time [1], therefore making the SSEP response easier to handle in comparison to the complex transient response which has a particular amplitude value at each point in time.

The electrical activity of the brain leads to an alteration of the hemodynamic response in terms of an increase of the cerebral blood flow. The mechanism that regulates the hemodynamic activity with respect to the electrical activity is called the neurovascular coupling. With its many unknowns, neurovascular coupling researches are very

popular because many questions about the reasons behind a diseased or an aging brain may be enlightened by understanding the workings of neurovascular coupling.

The electrical activity of the brain can be easily detected from the scalp by electroencephalography (EEG) with a very high temporal resolution in terms of milliseconds. Functional near infrared spectroscopy (fNIRS) is an optical technique to explore the hemodynamic changes that take place in the cortex. The fusion of EEG with fNIRS allows the simultaneous investigation of both the electrophysiological and the hemodynamic response of the brain to steady state visual stimulation.

1.2 Objectives

In this study, we investigate the stimulation frequencies to which the brain responds the most in terms of electrophysiological and hemodynamic response. We intend to determine the common stimulation frequencies, which both the electrophysiological and the hemodynamic response of the frontal lobe favor. We think that such a stimulation frequency may lead to a comparatively strong neurovascular coupling.

As the brain resonates at the driving stimulation frequency, the electrical and the hemodynamic activity of the cerebral cortex can be detected from the scalp. Although visual stimulation elicits the greatest response in the occipital cortex, it is possible to detect a widespread response from the other parts of the brain [2, 3, 4, 5, 6, 7, 8]. This study will focus on the ssVEPs measured from the occipital cortex and the frontal cortex by EEG as well as the hemodynamic response measured from the frontal cortex by fNIRS.

The ERP responses have small amplitudes and are embedded in the background EEG activity. When the event is visual stimulation, the ssVEP amplitudes detected elsewhere except from the occipital lobe are expected to be even smaller. Likewise, the hemodynamic response of the frontal lobe to visual stimulation is also expected to be very small which will make it hard to measure. Therefore, this study also explores the

limits of the fNIRS system in terms of its ability to detect the small changes that takes place on the frontal cortex in response to steady state visual stimulation.

1.3 Contributions of This Thesis

This thesis states that the ssVEPs detected from the occipital and frontal lobes peak at 9 and 12 Hz respectively. In the upper alpha band (10-13 Hz) and at 4 Hz frontal and occipital lobes exhibit close ssVEP power values.

This thesis also states that the cerebral oxygenation response of the frontal lobe due to visual stimulation can be detected by fNIRS. The cerebral oxygenation response of the frontal lobe peaks at 24 Hz.

We determined a positive and moderate linear correlation ($0.5 < r < 0.7$) between the electrophysiological and the cerebral oxygenation responses of the frontal lobe at 9, 12 and 20 Hz visual stimulation.

2. BACKGROUND

2.1 The Nervous System

The nervous system is composed of neurons (nerve cells) and glia. It is the biological information system of the body which is responsible for controlling all the biological processes and movement of the body. Environmental information is received, interpreted and responded via electrical signals by the nervous system. The nervous system is divided into two subsystems called the central nervous system (CNS) and the peripheral nervous system (PNS). CNS includes the brain and the spinal cord. The PNS consists of sensory nerves (afferent nerve) and motor nerves (efferent nerve) and it connects the CNS to the rest of the body. Sensory nerves receive sensory stimuli and feed information to the brain and the spinal cord, whereas motor nerves carry the messages of the brain and the spinal cord to the other parts of the body like muscles and organs.

2.2 The Nerve Cell

A nerve cell consists of a cell body called the soma, an axon and dendrites. The cell body of a neuron includes nucleus, mitochondria and other organelles which keep the nerve cell functioning.

The axon is a long, tubular extension of the cell which carries outgoing messages from the cell in the form of electrical impulses. The axon is surrounded by myelin sheath which has a knotty structure called the Nodes of Ranvier that speed up the electrical transmission. The axon ends up with the axon terminal bundle. Dendrites also extend from the cell body and they receive the impulses from the neighboring neurons. An electrical signal that is called the action potential is passed from the dendrites to the axon terminal bundle. Axon terminal bundle is a branched structure with ends called

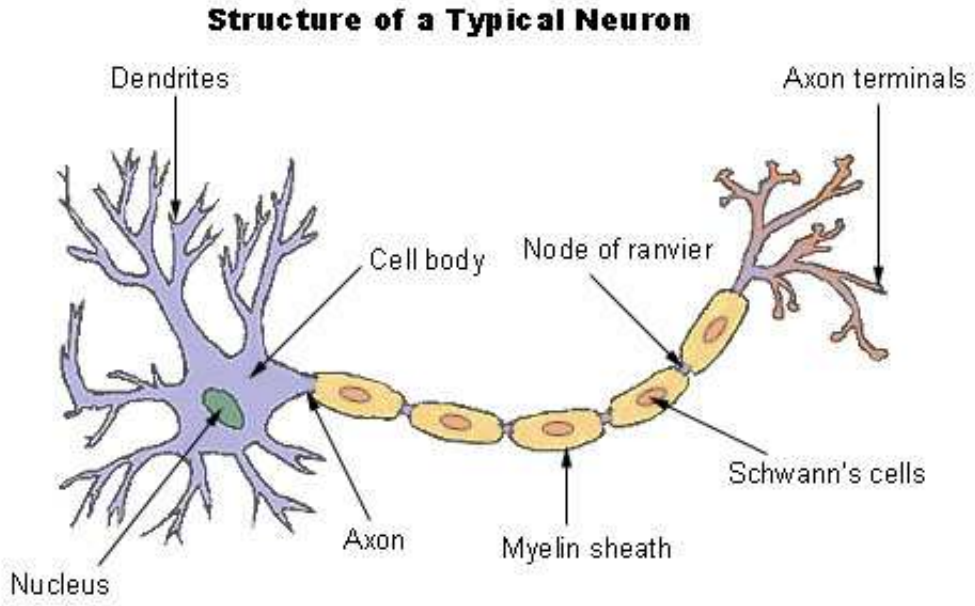

Figure 2.1 Structure of the nerve cell [9]

synaptic knobs. When electrical signal reaches the synaptic knobs of one neuron, neurotransmitters are released to the synaptic cleft. The neurotransmitter molecules bind to the receptors of the post synaptic neuron and causes changes in the membrane voltage distribution leading to the further transmission of the electrical signal.

Glial cells are the other main cell type of the nervous system and they constitute half the volume of the CNS. Unlike neurons glial cells don't conduct electrical signals. They surround neurons and provide support, protection, nutrition and oxygen for them. They insulate neurons from each other. Astrocytes, oligodendrocytes and microglia are the glial cell types of the CNS. Astrocytes are found in the brain capillaries and they are concerned with neurotransmission and neuronal metabolism. They restrict the substances that can enter the brain by forming the blood-brain barrier. Oligodendrocytes are involved in the myelin production by wrapping the neuronal axons. Microglia are involved in the immune system as they remove cellular waste and provide protection against pathogens and microorganisms. The glial cells of the PNS are known as Schwann cells. Schwann cells wrap the neuronal axons of the PNS forming a myelin sheath.

2.3 Brain Structure and Functional Organization

Brain and the spinal cord consist of white matter and gray matter. The white matter is made up of axons. It appears white because the axons are surrounded by myelin sheath which is a fatty material. The gray matter consists of cell bodies and dendrites. Cytoplasm of the cell bodies cause the gray matter to appear gray.

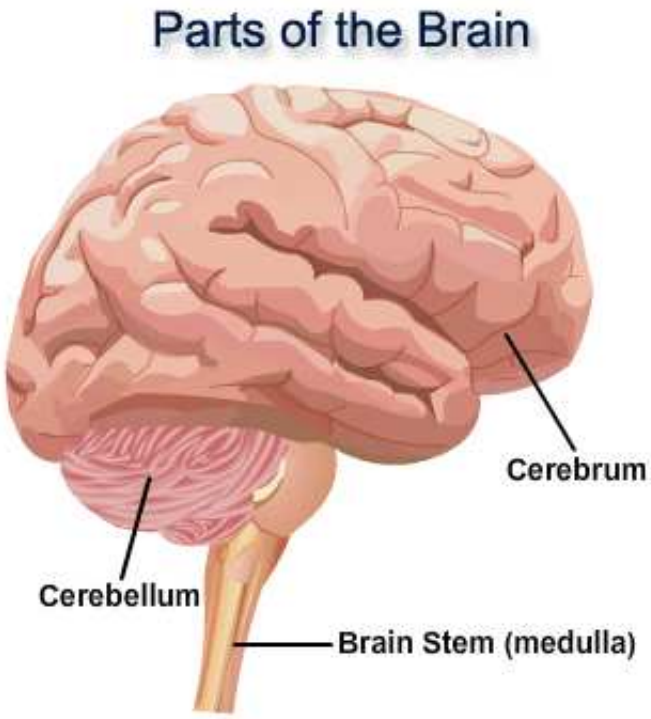

Figure 2.2 Major Parts of the human brain [10]

The human brain is divided into three parts called the brain stem (medulla), cerebellum and the cerebrum. The cerebrum or the cerebral cortex is the largest part of the human brain and has two halves that are mostly symmetrical, known as the left and right hemispheres. A bundle of axons called the corpus callosum connect the two hemispheres. Right hemisphere is associated with creativity and controls the left part of the body, whereas the left hemisphere is associated with logic and controls the right side of the body. Cerebrum is composed of gray matter at the surface layer and white matter at the inner layers. It is divided into four lobes: The frontal lobe, the temporal lobe, the parietal lobe and the occipital lobe.

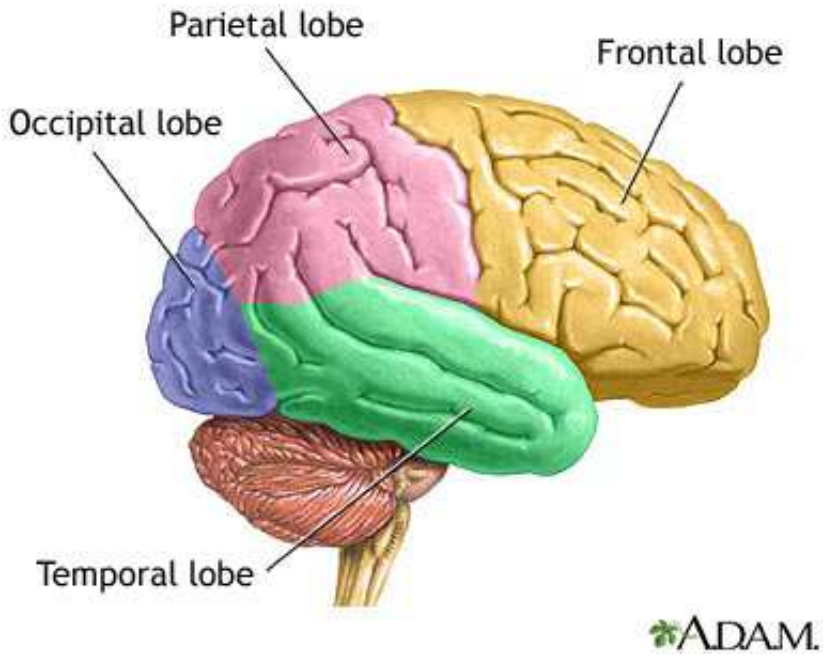

Figure 2.3 Lobes of the human brain [11]

Four lobes of the cerebral cortex also have specific functions. Frontal lobe is associated with reasoning, problem solving, planning, emotions and parts of movement and speech abilities. Temporal lobe is associated with speech, memory and auditory sense. Parietal lobe is associated with orientation, movement, recognition and stimuli perception. Occipital lobe is associated with visual perception.

Cerebellum is located at the lower back of the brain. It includes cardiac, vasomotor and respiratory centers and it is involved in coordination of balance and posture. Brain stem leads to the spinal cord and it consist of gray matter at the inside, surrounded by white matter. It is responsible for vital life functions such as breathing, blood pressure and heartbeat. It includes sensory pathways to body and face.

2.4 Brain Energy Metabolism

Changes in local brain energy metabolism can be studied in humans my monitoring alterations in glucose utilization, oxygen consumption, and blood flow during

activation of specific areas. 20% of total body oxygen consumption and %25 of total body glucose utilization is received by the brain. Glucose is the only physiological substrate for brain energy metabolism. Brain requires a continuous supply of oxygen in order to metabolize glucose and produce ATP. Neural activity is maintained by forming ionic gradients across the plasma membrane. Ionic pumps known as ATP-ase, Na+ and K+, that are located on the plasma membrane require energy in the form of ATP in order to maintain the electrochemical gradients.

Glycolysis and oxidative phosphorylation are the two mechanisms that produce ATP. Glycolysis is anaerobic process in which glucose is transformed into pyruvate and degraded to lactate without oxygen. 2 ATP molecules are produced during gycolysis. The aerobic energy production occurs in the citric acid cycle in which pyruvate is metabolized with oxygen, yielding 34 ATP molecules.

The oxygen carrier component of the blood is called hemoglobin. Hemoglobin molecule is composed of four globular protein subunits and a heme group. Heme group contains an iron atom that can bind an oxygen molecule.

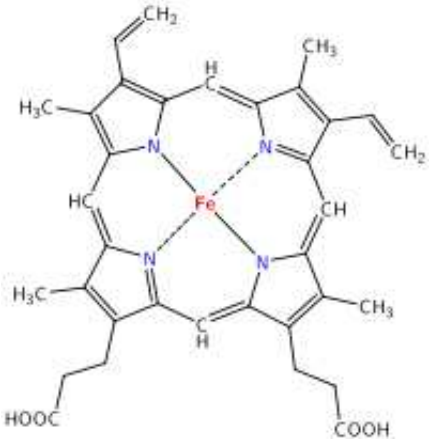

Figure 2.4 Hemoglobin molecule [12]

Hemoglobin molecule gives the red blood cells its red color. Oxygen bounded hemoglobin is called oxyhemoglobin [HBO2] and hemoglobin without an oxygen bound is called deoxyhemoglobin [HBO].

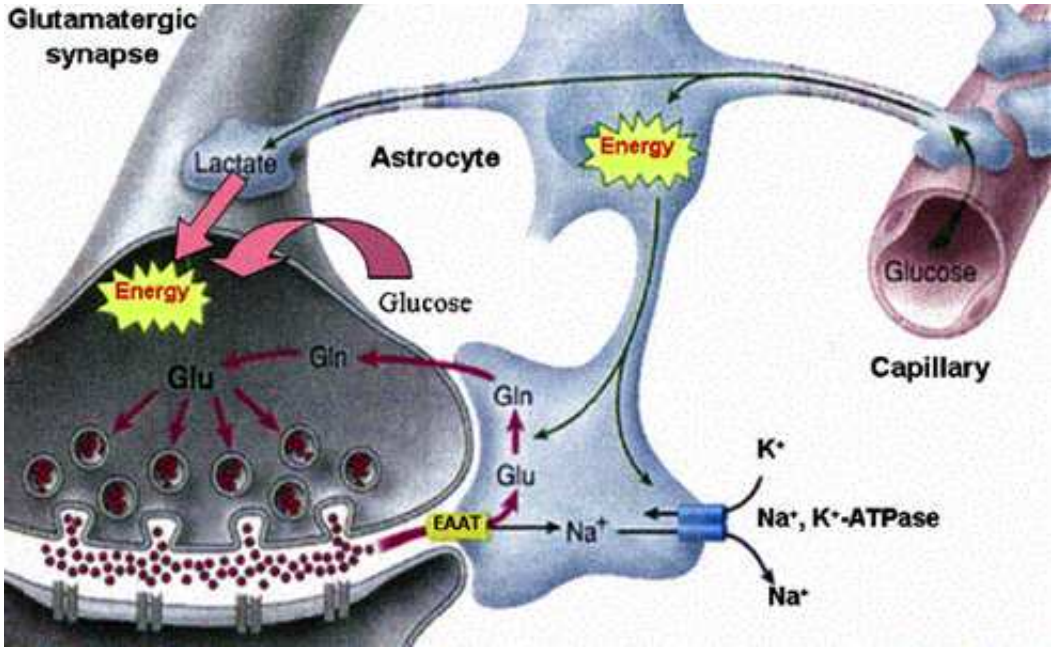

Figure 2.5 Illustration of the astrocyte-lactate shuttle [13]

Astrocytes that surround brain capillaries play an important role in brain energy metabolism. Glucose enters the brain from the arterial side and is predominantly taken up by astrocytes, which then transform it to lactate by glycolysis. Lactate exchange occurs between astrocytes and neurons. Astrocytes release lactate into the extracellular space and neurons take up the lactate to oxidize it aerobically during neural activity. The emerging CO2 and H2O are drained by the venous blood.

2.5 Neurovascular Coupling

Cerebral metabolism depends on a constant supply of glucose and oxygen. Continuous supply of these energy substrates are maintained by cerebral blood flow (CBF). Neurovascular coupling refers to the relationship between local neural activity and subsequent changes in CBF. Neurovascular coupling mechanism is still not fully understood. According to Roy and Sherrington, cerebral blood flow is controlled by energy demand [14]. Variations in the concentrations of metabolic by-products (CO2, K+, H+) may change the polarization of the vascular smooth muscle cells and trigger vasodilation or vasoconstriction. On the other hand Attwell and Iadecola and Lauritzen

state that cerebral blood flow is controlled by neural signaling via neurotransmitters [15,16].

Neural activation leads to an increase in cerebral blood flow but oxygen consumption is less than the cerebral blood flow. Functionally induced focal cortical hyperoxygenation results from an increase in regional cerebral blood flow (rCBF), which is not coupled to a proportionally large increase in oxygen consumption (CMRO2) [17, 18]. This mismatch leads to an increase in oxyhemoglobin and to a decrease in deoxyhemoglobin and results in a total increase in total hemoglobin (tHB). CBF lags behind the neural activation by 1-2 seconds and reaches its maximum in approximately 5 seconds after the neural activation.

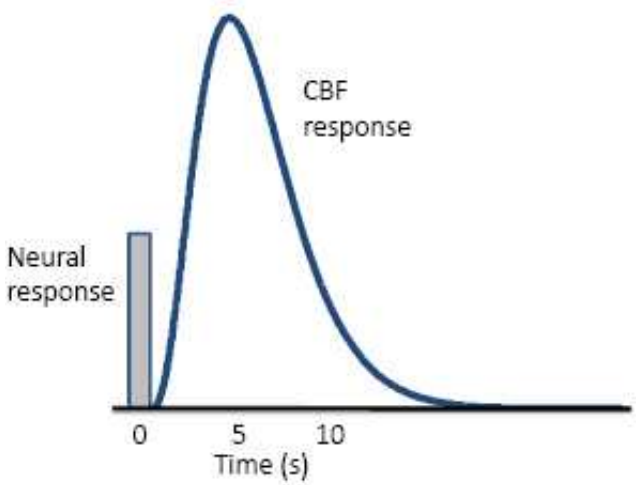

Figure 2.6 Coupling of CBF response to neural activation in time [19]

Neurovascular coupling may be altered under abnormal physiological conditions such as those found in the diseased or aging brain. Diseases such as hypertension, diabetes and Alzheimer may lead to abnormal patterns of vasodilation after neural activation. Aging may reduce the elasticity of blood vessels and therefore affect vasodilation and vasoconstriction. Neural injuries may also lead to impaired neurovascular coupling. Hence mastering the dynamics of the neurovascular coupling may offer an alternative method for the diagnosis of such anomalies.

2.6 Steady State Visual Evoked Potentials

The term evoked related potential (ERP) was first used by Herb Vaughan (1969). Evoked related potentials are electrical potentials recorded from the nervous system that are evoked by stimuli. ERP is the electrical activity of the brain related to a sensory, motor or cognitive event. ERP technique is used in brain mapping and cognitive neuroscience studies.

There are two main types of electrical activity associated with the neurons, action potentials and postsynaptic potentials [20]. Action potentials are in the form of discrete voltage spikes that travel through the axons. Postsynaptic potentials are generated when the neurotransmitters bind to the receptors of the postsynaptic cell. Action potentials in different axons typically cancel and the duration of an action potential is only about a millisecond. On the other hand, postsynaptic potentials last tens to hundreds of milliseconds and when the postsynaptic potentials of many neurons summate, it is possible to measure the resulting voltage at the scalp. In order to record the synchronous activity of millions of neurons, the spatial orientation of these synchronously firing neurons must be the same and radial to the scalp. Therefore evoked related potentials reflect postsynaptic potentials rather than action potentials.

Visual evoked potential (VEP) is used to describe ERPs elicited by visual stimuli. Visual stimuli can be in terms of flashing lights or flickering checkerboard patterns. VEP applications are very useful for detecting blindness or for the diagnosis of optic neuritis and multiple sclerosis. VEP is widely used in visual perception investigations.

Steady state evoked potentials (SSEP) are generated in response to repetitive sensory stimulation in which the constituent frequency components of the response remain constant with time in both amplitude and phase [1]. SSEPs are composed of the superposition of the complex transient responses of each singular stimulus. The system resonates at the stimulus rate and its multiples. Typicaly, steady state responses look like two summed sine waves, one at the stimulation frequency and one at twice the stimulation frequency [20]. Therefore the steady state response can be summarized

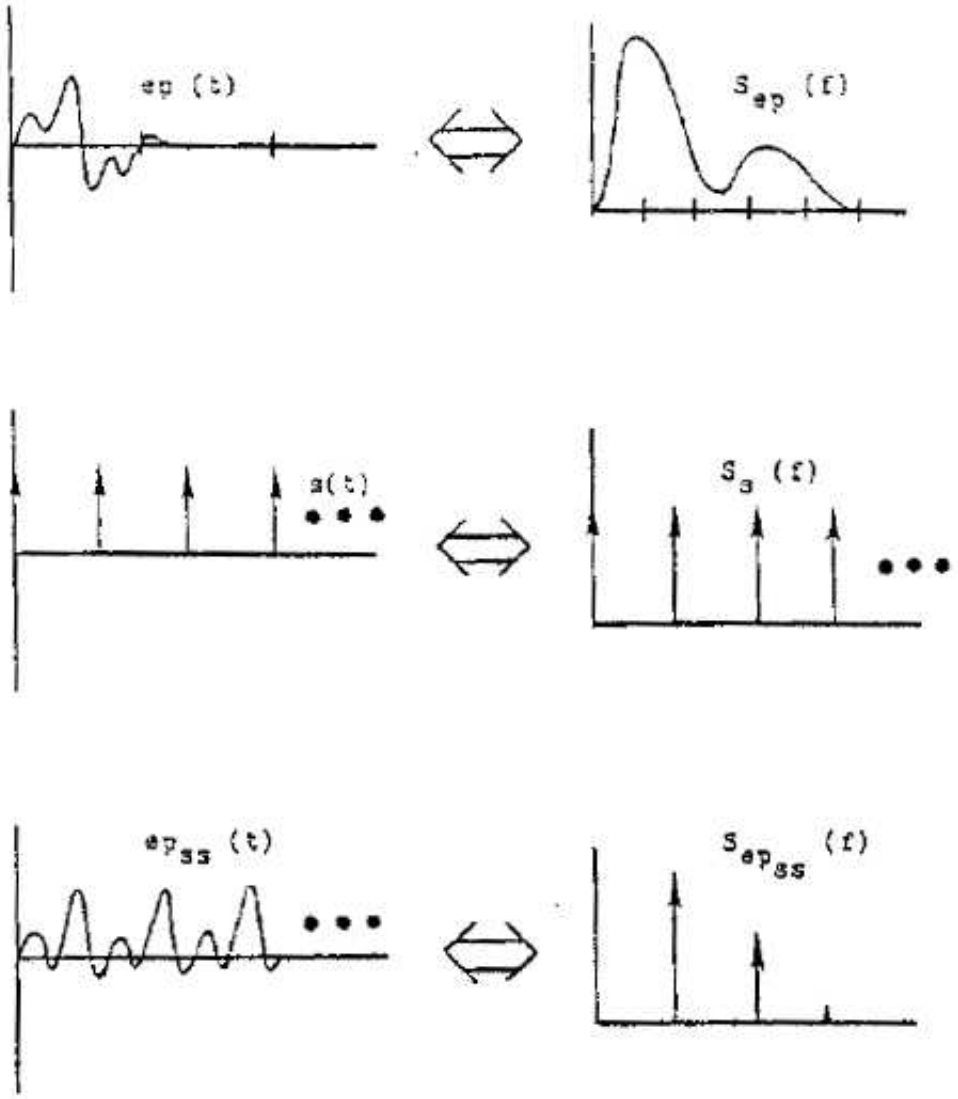

Figure 2.7 Time and frequency domain representation of the EP in response to single and repetitive stimulation [21]

by the amplitudes and phases of each of the sine waves, whereas transient responses have seperate amplitude values at each point in time.

$$ssep(t) = ep(t) * s(t) \tag{2.1}$$

$$S_{ssep}(jw) = S_{ep}(jw).S_s(jw) \tag{2.2}$$

In equations 2.1 an 2.2, $ep(t)$ is the single evoked response, $s(t)$ is the impulse train and $ssep(t)$ is the steady state evoked response. "$*$" stands for the convolution operator. $S_{ssep}(jw)$, $S_{ep}(jw)$ and $S_s(jw)$ are the frequency domain representations of the $ep(t)$, $s(t)$ and $ssep(t)$.

2.7 Signal Averaging

Evoked potentials are time locked as they occur at specific latencies from presentation of the stimulus. Evoked potentials have low magnitudes, therefore in order to distinguish them from the backround EEG activity, which has an amplitude of about 10 to $100\mu V$, a large number of identical stimuli must be applied. Evoked potentials can be extracted from the recorded EEG activity by signal averaging. Signal averaging is performed on multiple trials with the same duration. In this case each trial is composed of a spontaneous EEG acivity which is assumed to be random noise and an evoked potential, therefore if very large number of trials are averaged, the random noise will be totally removed .

$$R_{av} = (1/\sqrt{N}).R \tag{2.3}$$

In equation 2.3, R is the amount of noise on a single trial, R_{av} is the amount of noise on the averaged signal and N is the number of trials.

Accordingly, when the signal is averaged, noise decreases as a function of the square root of the number of trials, in other words, the signal-to-noise (S/N) ratio increases as a function of the square root of the number of trials.

3. NEUROIMAGING TECHNIQUES

3.1 Functional Near Infrared Spectroscopy (fNIRS)

Near infrared spectroscopy (NIRS) is a non invasive optical imaging technique that is used to investigate regional hemodynamics. In 1977, Jöbsis demonstrated that blood flow and tissue oxygenation can be estimated in vivo depending on the differential absorption of NIR light by hemoglobin, oxyhemoglobin and cytochrome C oxidase [22]. Human brain can be optically imaged by NIRS because near infrared light (650-950nm) is able to penetrate the scalp and scull and can be attenuated by the tissue. As HB and HBO2 have different absorption characteristics and as absorption of near infrared light is proportional to the concentrations of HB and HBO2 present in the tissue, changes in regional cerebral blood volume and oxygenation can be determined by detecting the absorbed light intensity. Beer-Lambert Law describes the attenuation of light in non-scattering a medium:

$$A = \log_{10}(I_0/I) \tag{3.1}$$

$$\log_{10}(I_0/I) = \epsilon(\lambda).l.C \tag{3.2}$$

$$A = \epsilon(\lambda).l.C \tag{3.3}$$

In equation 3.1, A is the absorbance of the compound, I_0 is the incident light intensity and I is the transmitted light intensity. In equations 3.2 and 3.3, $\epsilon(\lambda)$ is the molar absorption coefficient as a function of wavelength ($Lmol^{-1}cm^{-1}$), l is the optical path length through the medium or the source-detector distance (cm) ad C is the concentration of the compound ($molL^{-1}$).

Beer-Lambert Law states that the optical absorbance of a compound in a non-scattering and non-absorbing medium varies linearly with both the compound concentration present in the medium and the optical path length. The optical path length is determined by the distance between the source and the detector and the greater the path length the greater the chance of absorption occurring and vice versa [23].

Attenuation of NIR light in tissue occurs in two ways: Absorption and scattering. The compounds that absorb light in a specific range of the optical spectrum are called chromophores. Melanin, water, lipids and hemoglobin are the basic chromophores of the tissue. The chromophores of the tissue have different absorption characteristics; they absorb light at different wavelengths. Melanin is a pigment found in the epidermal layer of the skin and it strongly absorbs ultraviolet light. Water is abundant in biological tissue and its absorption spectrum is the same with the absorption spectrum of lipid. In NIR region, water absorbs less than hemoglobin does. This absorption feature of water creates a transparency window of biological tissue which allows deeper penetration of NIR light and spectroscopic measurement of hemoglobin. The absorption of HB and HBO2 in NIR region is not as high as it is in the visible region but NIR region allows the spectroscopic separation of these two chromophores because in the NIR region their absorption spectra significantly differ.

Optical imaging of the brain is possible for a limited region. Light has to penetrate through skin, skull, cerebrospinal fluid and reach the cerebral cortex, however biological tissue is highly scattering. Scattering occurs at the interface of two different media with different optical properties such as the membrane boundaries of the cells. Each layer has different optical properties. Skin and skull have high scattering properties but cerebrospinal fluid has low scattering properties and it allows the pen-

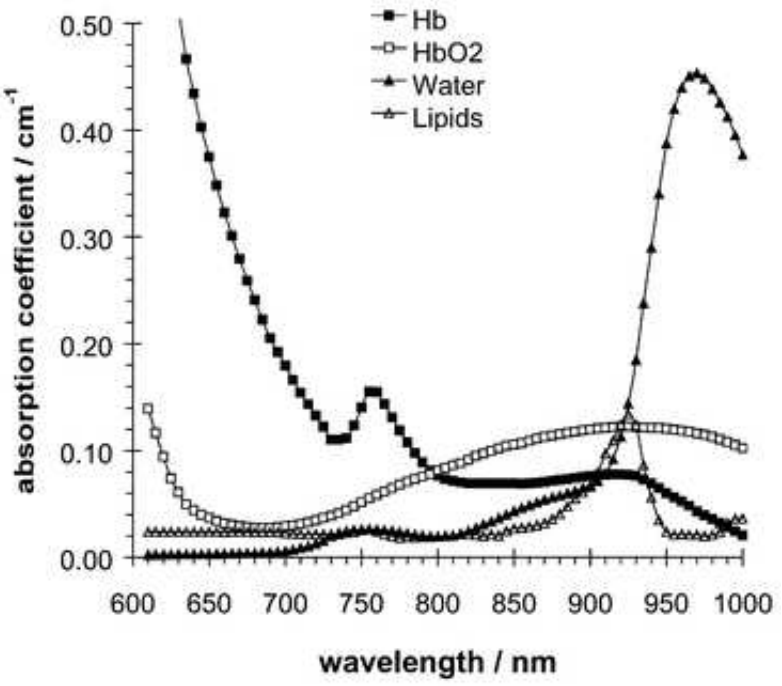

Figure 3.1 The absorption spectra of chromophores [24]

etration of light to the gray matter of the cerebral cortex. However cerebral cortex is also highly scattering and only few photons can reach the white matter. Near infrared spectroscopy is interested in only the amount of the absorbed light in order to calculate the concentration of the absorber, however it is impossible to distinguish the light attenuation due to absorption from the attenuation due to scattering, therefore NIRS makes use of the modified Beer-Lambert's Law which amends this incompleteness.

$$A = \epsilon(\lambda).l.C.B(\lambda) + G \tag{3.4}$$

In equation 3.4, $B(\lambda)$ is the differential path length factor and G is the signal loss due to light scattering.

G depends on the geometry and the scattering coefficient of the tissue. Since G is unknown, the absolute concentration of the chromophore and the absolute attenuation cannot be found, however G is constant throughout the measurements, therefore change

in chromophore concentration can be found from the change in attenuation.

$$A(t_0, \lambda) = C(t_0).\epsilon(\lambda).l.B(\lambda) + G \tag{3.5}$$

$$A(t_1, \lambda) = C(t_1).\epsilon(\lambda).l.B(\lambda) + G \tag{3.6}$$

$$\delta A(\lambda) = A(t_1, \lambda) - A(t_0, \lambda) \tag{3.7}$$

$$\delta A(\lambda) = \delta C.\epsilon(\lambda).l.B(\lambda) \tag{3.8}$$

$$\delta c = \delta A(\lambda)/[\epsilon(\lambda).l.B(\lambda)] \tag{3.9}$$

In equations 3.5, 3.6 and 3.7, t_0 is the start time of the measurement and t_1 is the end time of the measurement.

Total hemoglobin (tHB) or blood volume (BV) change and oxygenation (Oxy) change can be calculated:

$$\Delta[BV] = \Delta[HBO2] + \Delta[HB] \tag{3.10}$$

$$\Delta[Oxy] = \Delta[HBO2] - \Delta[HB] \tag{3.11}$$

NIRS can be used for the detection of the illnesses concerning the blood circulation system and for the investigation of vascular changes due to neural activation. NIRS systems are cheaper in comparison to other modalities that are used in monitoring hemodynamic activity since they have simple technical equipment. As they are portable devices, they can be implemented in any experimental environment and in any experiment that requires the free movement of the subject. NIRS is noninvasive and depends on non-ionizing radiation, for this reason it can be applied on infants and children and on subjects that cannot undergo an fMRI or PET examination.

3.2 Electroencephalography (EEG)

Electroencephalography (EEG) is a technique for recording the electrical activity of the brain by placing electrodes on the scalp, amplifying the signal and plotting the changes in voltage over time. EEG technique was found by a German scientist Hans Berger (1929).

EEG signal is the summation of the postsynaptic potentials of millions of synchronously firing neurons with the same spatial orientation that are radial to the scalp surface. This is most likely to occur in cortical pyramidal cells, which are aligned perpendicular to the surface of the cortex [20]. The individual currents generated by the postsynaptic potential of a single neuron can be represented by a dipole. EEG measures the summation of spatially aligned dipoles from many neurons. Since the

cortex has a folded structure, the summation of the individual dipoles is complicated. The equivalent current dipole (ECD) which is the summation of many dipoles is found by averaging the orientations of the individual dipoles.

Brain is a conductive medium and a conductive medium conducts the current present in it throughout the medium until it reaches the surface. Therefore a current dipole that resides in the brain generates an electrical potential distribution on the scalp surface. If the locations and the orientations of the set of dipoles in a volume conductor with a known conductance are known, it is possible to estimate the electrical potential distribution on the surface of the conductor that is generated by the set of dipoles. Estimating the voltage distribution on the surface by looking at the source is called the forward problem. On the other hand it is a much more complicated task to estimate the locations and the orientations of a set of dipoles that resides in a volume conductor by looking at the measured voltage distribution on the conductor surface. Estimating the source by looking at the voltage distribution on the surface is the concern of the inverse problem. Solving the inverse problem is more challenging since there is not just one dipole configuration that is responsible for the observed voltage distribution.

Different states of brain functioning leads to characteristic EEG wave forms that oscillate at particular frequency ranges. These rhythmic changes are categorized into four basic groups: Alpha, beta, theta and delta waves. Alpha waves (8-12 Hz), beta waves (12-30 Hz), theta waves (4-7 Hz) and delta waves (up to 4 Hz). EEG wave forms are associated with various states of consciousness. Alpha waves are observed when a person is relaxed and drowsy. Beta waves are observed when a person is fully awake and alert. Theta waves are associated with creative thinking and mediation. Delta waves are related to deep, dreamless sleeping and they are the slowest wave types with the highest amplitude. EEG activity can also be observed in transient forms such as spikes, sharp waves, vertex waves and sleep spindles. Spikes and sharp waves may arise from various disorders such as epilepsy; therefore EEG records are clinically used to detect epileptic seizures. EEG is also used to monitor anesthesia depth, to detect brain damage and brain death and to diagnose tumors, stroke and coma.

EEG measurements can be affected by biological and environmental artifacts. Biological artifacts may generate from eye movements, clenching of jaw muscles, cardiac activity, and respiration or even from sweating. Unproper grounding of the EEG electrodes may also lead to 50/60 Hz noise. However various artifact reduction and source separation techniques are available to remove EEG artifacts.

EEG is weak in terms of spatial resolution due to the source localization problems and the voltage blurring effect of the skull caused by its high resistance. But the main advantages of EEG technique are its low cost, noninvasiveness and high temporal resolution.

3.3 Multimodality Neuroimaging Approach and EEG-fNIRS Fusion

Various neuroimaging techniques have various spatial and temporal resolution properties and limitations which affect the imaging quality. Multimodal neuroimaging approaches merge various imaging modalities with different advantages and disadvantages to compensate for each others limitations and to create a new imaging modality with reinforced spatiotemporal characteristics.

Neuronal activity causes electrical and hemodynamic changes. Neurovascular coupling investigations require the examination of both activity types. Multimodal neuroimaging allows the simultaneous monitoring of both electrical and hemodynamic activity and make it possible to investigate the correlations between electrophysiological, hemodynamic and metabolic changes.

Fusion of EEG and fNIRS aims the simultaneous measuring of hemodynamic and electrophysiological changes in the brain associated with neural activity. EEG has high temporal resolution in terms of milliseconds but the spatial resolution of EEG is poor. EEG measures the electrical potentials on the scalp by placing electrodes on the

scalp but the locations of the source dipoles that create the electrical potential on the scalp can not be exactly determined. fNIRS can partially replace for fMRI because it detects HBO2, HB and thus the total hemoglobin (tHB) concentration changes which substitutes for the fMRI's BOLD signal . It is a non-invasive imaging technique and employs non-ionizing radiation, thus can be used on infants conveniently unlike fMRI. fNIRS systems are also more portable, cheaper and easier to implement in comparison to fMRI. Measurements can be taken even from moving subjects. However fNIRS can only scan the cortical tissue, while fMRI can scan the whole brain.

4. METHODS

4.1 Subjects and Experimental Procedure

13 healthy subjects (7 male and 6 female) at the average age of 26.46 participated in this study. Consents were obtained from all subjects and they were all informed about the study before the experiment. The experiments were performed in the EEG lab of the Physiology Department of Istanbul University Medical Faculty.

EEG and fNIRS measurements were conducted simultaneously. Subjects were seated in a dimly illuminated, insulated room and they were told to look at a focal point in front of them. Meanwhile they were exposed to visual stimuli at 26 different frequencies: 4, 5, 6, 7, 8, 9, 10, 11, 12, 13, 14, 16, 18, 20, 22, 24, 26, 28, 30, 32, 34, 36, 38, 40, 42 and 44Hz. The visual stimuli were introduced randomly.

The experiment started and ended with one minute long rest periods. Each stimulation frequency was introduced as two consecutive blocks of 30 seconds and each 30 seconds long stimulation period was followed by 45 seconds long rest period. In this manner the whole experiment lasted 67 minutes.

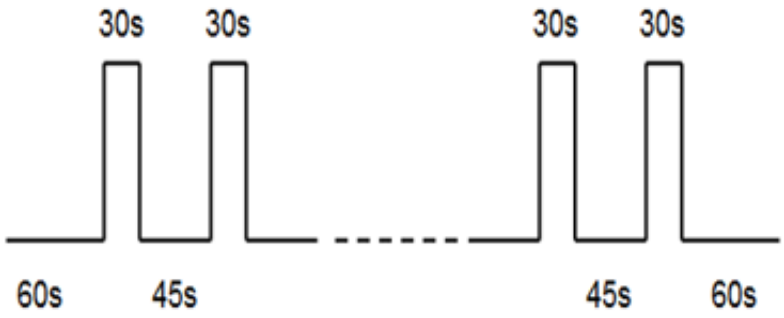

Figure 4.1 Experimental protocol

4.2 Stimulation System

Visual stimulation was applied by 4 LEDs of 1W power. The stimulation timing was controlled by NI-DAQ 6218 USB card. In order to keep the light energy at each applied stimulation frequency, the duty cycle was determined to be 50%. Light was reflected on a diffusive screen which was positioned 1 meter away from the subject.

4.3 fNIRS Equipment

The fNIRS system (NIROXCOPE 301) was developed at the Biophotonics Laboratory of Boğaziçi University. NIROXCOPE 301 has a sampling frequency of 1.77 Hz and it consists of the data acquisition unit, data collecting computer and a flexible probe to place on the foreheads of the subjects. NIRS can be implemented by time resolved, frequency domain and continuous wave techniques [25]. NIROXCOPE 301 is a continuous wave NIRS system. In continuous NIRS systems, light with constant amplitude is injected to the tissue and amplitude decay of the light intensity due to absorption is analyzed [26].

NIROXCOPE 301 system was designed to work as two parallel systems in order to monitor the right and the left hemispheres for functional studies at the same time. On the probe there were 2 light emitting diodes which emit light at multiple wavelengths in the near infrared range: 730 nm, 805 nm and 850 nm. 730 nm is highly absorbed by HB and 850 nm is highly absorbed by HBO2, whereas 805 nm is equally absorbed by both chromophores. The concentrations changes of the chromophores were calculated by depending on the modified Beer Lambert Law.

The probe has 8 photodetectors that is sensitive to the wavelengths of 730 nm, 805 nm and 850 nm. The photodetectors detects the light that is reflected by the tissue. The 2 LEDs and 8 photodetectors are embedded in a soft covering on the probe.

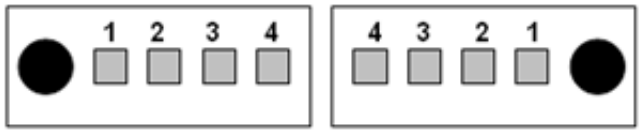

Figure 4.2 Source-detector locations of the NIROXCOPE 201

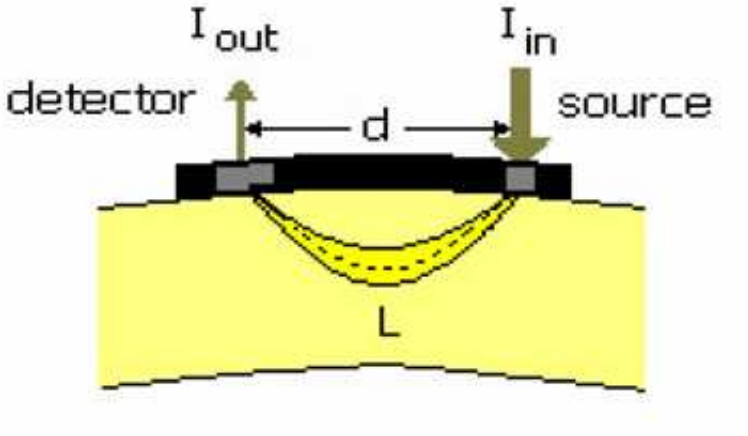

Figure 4.3 Illustration of the optical pathway in NIRS imaging

As light is emitted by the LEDs, some of the photons are absorbed by different layers of the tissue such as the skin, skull and the brain. The remaining photons exit the head after following a banana shaped pathway throughout the tissue between the LEDs and the detectors due to scattering effect of the tissue [27]. The backscattered photons are captured by the detector. The distance between the source and the detectors varies depending on the location of the detectors on the probe. The inter detector distance is 1 cm, and the nearest detectors are 1 cm away from the LEDs. In this experiment the data obtained from the thirdly detectors which were 3 cm away from the LEDs were used. In this manner a penetration depth of at least 1.5 cm in the tissue was reached allowing the investigation of the first few millimeters of the gray matter.

4.4 EEG Equipment

EEG measurements were recorded by the 32 channel BrainAmp MR+ amplifier (BrainProducts Inc, Munchen, Germany). EEG electrodes were places on the scalp by

an electrode cap that is designed according to the international 10-20 lead system.

The 10-20 system is a specific electrode placement system. Electrodes are placed at specific locations along the head, with specific intervals. Total front-back and right-left distances of the skull are measured by taking some bony landmarks as reference points. These bony landmarks are the inion, the nasion and the preauricular points. Inion is the bump at the back of the head; nasion is the point between the nose and the forehead and the preauricular points denotes the lymphatic nodes in front of the auricles of the ears. '10' and '20' refer to the 10% and 20 % inter electrode distances. The distance between the inion and nasion and the distance between the preauricular points are measured and the electrodes are placed by %10 and %20 inter electrode distances on the lines that connect the bony landmarks.

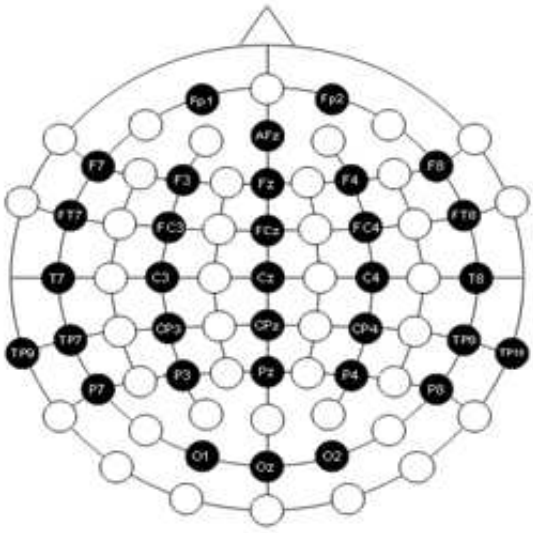

Figure 4.4 Electrode locations on the head model according to the international 10-20 lead system

The electrode names are: Fp1, Fp2, Afz, F3, Fz, F4, F8, FT7, FC3, FCz, FC4, FT8, T7, C3, Cz, C4, T8, TP7, CP3, CPz, CP4, TP8, P7, P3, Pz, P4, P8, O1, Oz and O2. The letters indicate the lobes and the numbers indicate the hemispheres of the brain. The letter F stands for the frontal lobe, T, P, C and O stands for the temporal, parietal, central and occipital lobe. The letter Z refers to an electrode that is placed on the midline. Even numbers refer to the right hemisphere and odd numbers refer to

the left hemisphere. The smaller the number, the closer the electrode position is to the midline.

In EEG systems high pass and low pass filters are used in order to attenuate the effects of large voltage shifts due to skin potentials and to attenuate the noise related high frequencies. The signals were analog filtered between 0.1-250 Hz and sampled at 1000 Hz. The time constant was determined to be 10s. Ag/AgCl disc electrodes were used and the electrodes were connected to the skin by electrode gel and electrode paste. Electrode connections were made unipolar and impedance values of the electrodes were kept under 10kΩ. The average potential of both earlobes were determined to be the electrical reference and the left earlobe served as the ground point. Differential amplifiers are used in EEG systems for EEG amplification. Differential amplifiers amplify the difference between the active electrode-ground voltage and the reference-ground voltage to eliminate any noise that is present in the ground and to obtain clean EEG recordings.

Records were taken from 29 channels (Afz, F3, Fz, F4, F8, FT7, FC3, FCz, FC4, FT8, T7, C3, Cz, C4, T8, TP7, CP3, CPz, CP4, TP8, P7, P3, Pz, P4, P8, O1, Oz, O2). Fp1 and Fp2 electrodes were not placed on the forehead because the fNIRS probe covered the forehead instead.

5. DATA ANALYSIS

5.1 Analysis of the EEG Data

Evoked related potentials (ERPs) are embedded in the EEG signal and in order to embody the ERPs and minimize the EEG noise, signal averaging is needed. Each EEG trial contains an ERP waveform and random noise. The noise is assumed to be random because it is not related to the time locking event and ERP waveform is assumed to be identical for each trial. To average the trials that belong to the same event, in this case to the same stimulation frequency, EEG epochs following the stimulus are extracted and aligned with respect to the time locking stimulus and these epochs are then averaged. The EEG epochs are designated to be 1 second long.

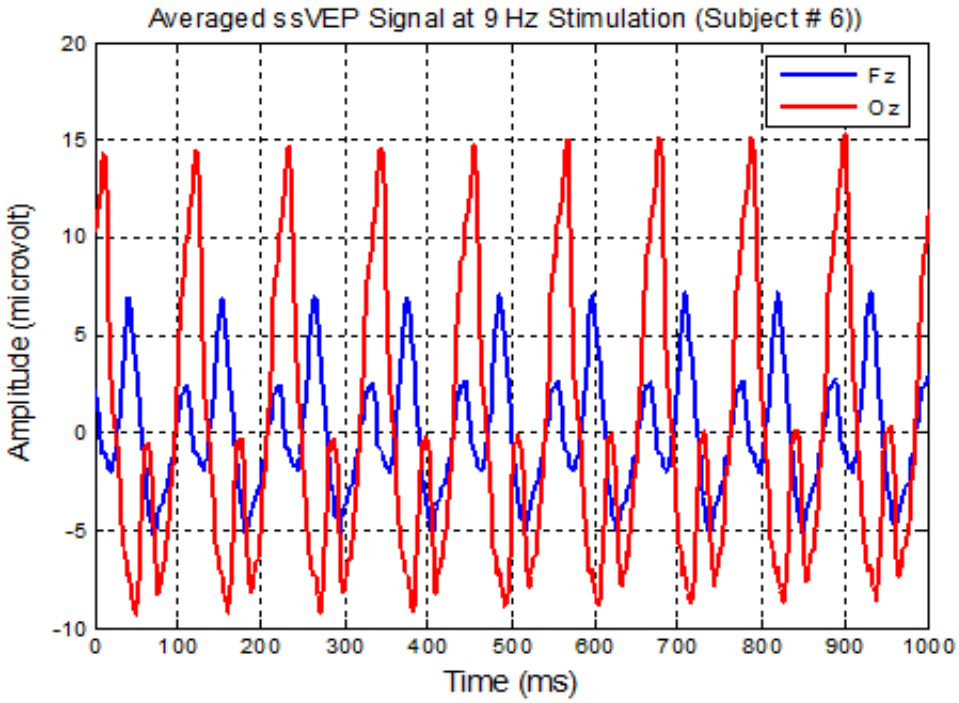

Figure 5.1 Time averaged ssVEP signal recorded in response to 9 Hz stimulation

In Figure 5.1, one second long time averaged ssVEP response of the 6th subject in response 9 Hz stimulation frequency is demonstrated. The amplitude of the ssVEP response recorded from the Oz electrode which corresponds to the occipital cortex is

greater than the ssVEP response recorded from the Fz electrode which corresponds to the frontal cortex. Nine consecutive peaks of sine waves, one for each flashing of the light, can be distinguished from the above graph. The ssVEP response is composed of two summed sine waves, one for the stimulation frequency and other for twice the stimulation frequency.

After signal averaging is performed, the power spectral density of the resulting average EEG epoch is calculated for each stimulation frequency. Welch's averaged modified periodogram method of spectral estimation was used in power spectral density calculations. 1000 data point long EEG signal was segmented with 50% overlap and each segment was windowed by a 1000 point Hamming window. 1000-point Fast Fourier transform was applied to the windowed signal segments. Then the periodogram of each segment is computed and the average of the periodograms was calculated to form the spectrum estimate. Lastly the spectrum estimate is scaled by the sampling frequency and the power spectral density is found as a result.

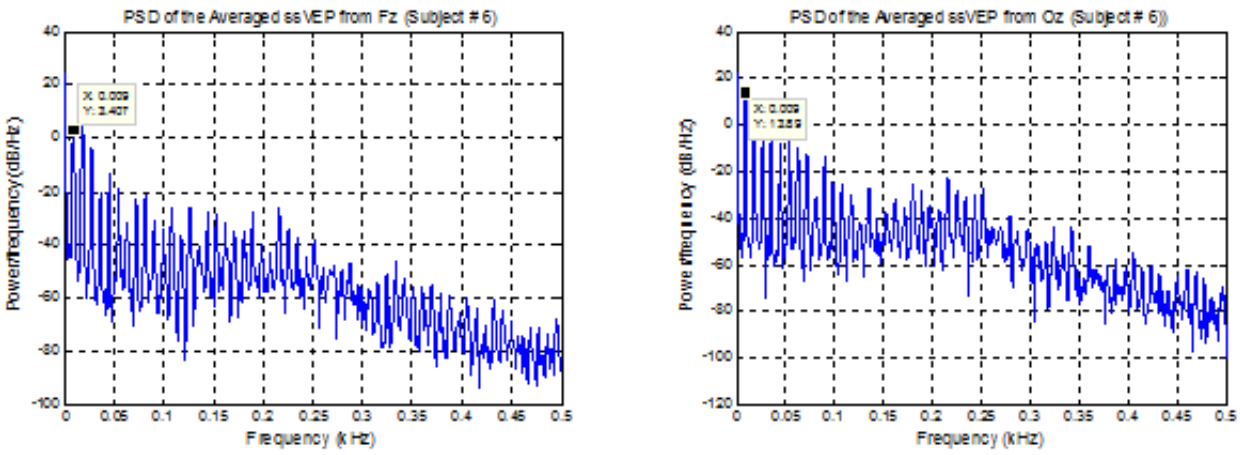

Figure 5.2 PSD of the time-averaged ssVEP signal recorded from the a) frontal region b) occipital region of the 6th subject during 9 Hz stimulation

The power spectral density analysis of the time averaged ssVEP signals reveal the power distributions of the stimulation frequencies and their harmonics. In Figure 5.2 the power distribution of the time averaged ssVEP signal recorded from the 6th subject in response to 9 Hz is demonstrated. The power is maximal at the fundamental

frequency (stimulation frequency) for the frontal region recordings obtained from the Fz electrode, whereas it is maximal at the second harmonic of the stimulation frequency for the occipital region recordings obtained from Oz electrode. Besides the power values of the stimulation frequency at 9 Hz, the power values at its harmonics at 18, 27, 36 Hz and so on can also be easily distinguished in Figure 5.2.

The EEG records obtained from the frontal electrodes AFz, Fz, F3, F7, F4, F8 and occipital electrodes O1, O2 and Oz were used in this study. The average of F3 and F7 and the average of F4 and F8 calculated which were assumed to represent the left and the right hemispheres respectively. The central frontal electrodes AFz and Fz were also averaged. The averages of all the frontal electrodes and the occipital electrodes were also calculated in order to investigate the distributed ssVEP responses of the respective regions.

5.2 Analysis of the fNIRS Data

The signals obtained from the thirdly detectors were used in this study. HBO2 signals were analyzed. The recorded signal was band pass filtered in order to remove the baseline shifts and high frequency oscillations. The band pass filter was a 4th order Butterworth filter with the cut-off frequencies 0.01-0.05 Hz.

In order to determine the cut-off frequencies of the band pass filter, firstly Fast Fourier Transform analysis was performed on the recorded raw HBO2 signal. The 4096 point Fast Fourier Transform analysis revealed that the frequency components with the highest energy concentrate around 0.01-0.05 Hz range.

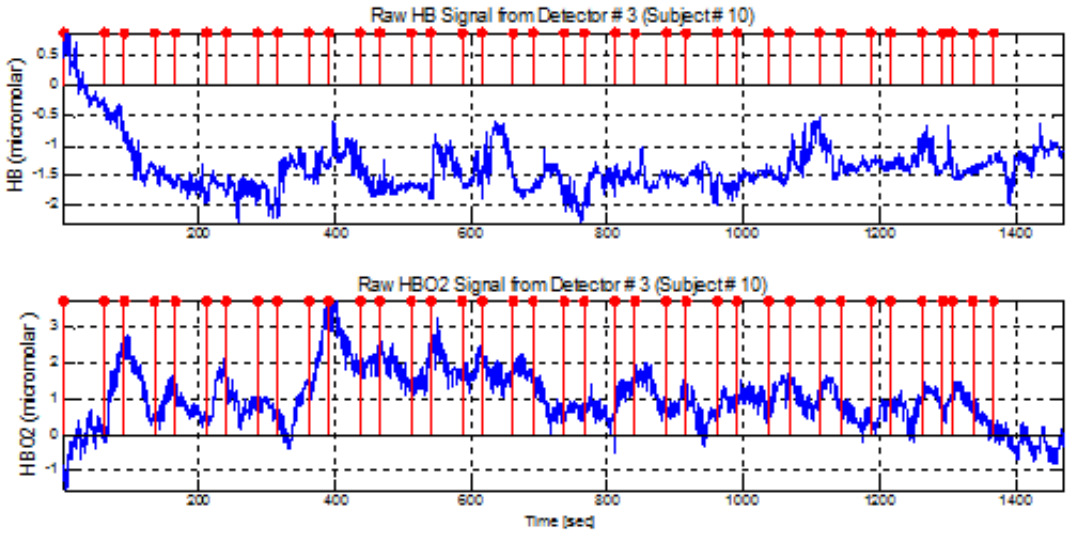

Figure 5.3 HB and HBO2 signals obtained from the 3. detectors of the NIROXCOPE 201 probe (Subject # 10)

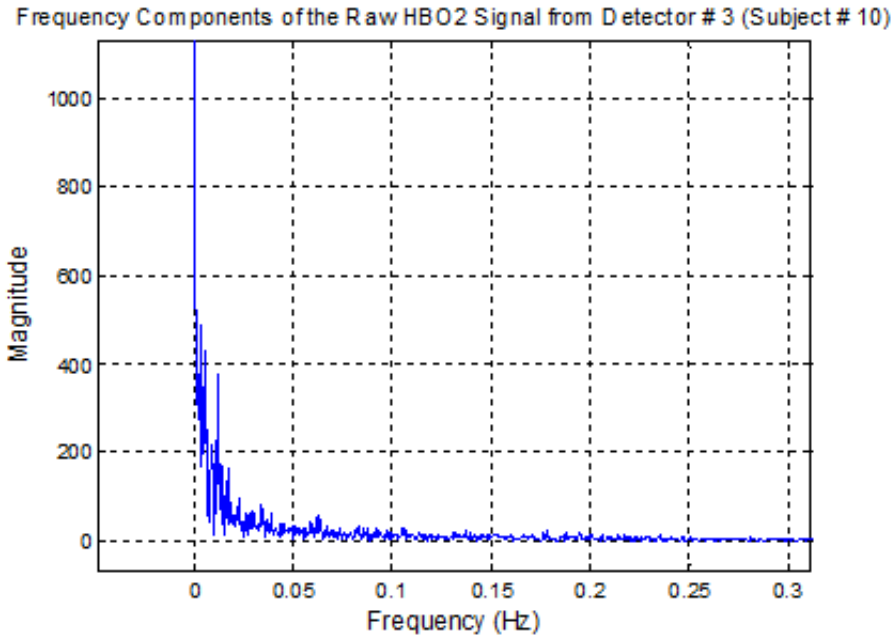

Figure 5.4 Frequency components of the raw HBO2 signal

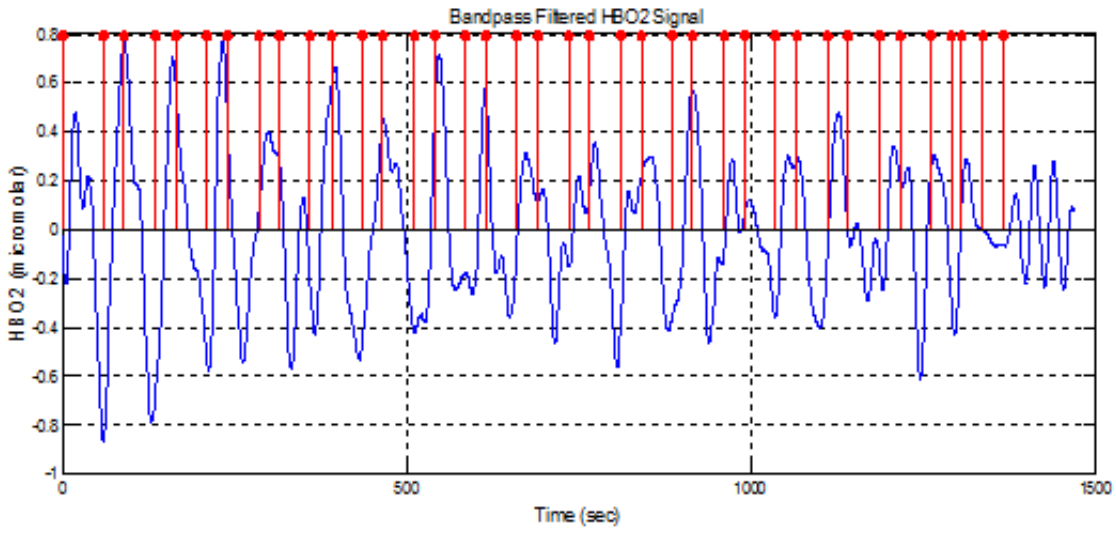

Figure 5.5 Band pass filtered (4th order Butterworth filter with cutoff frequencies of 0.01-0.01 Hz) HBO2 signal

Amplitudes of the HBO2 signals recorded during stimulation were measured with respect to the baseline which is assumed to be zero. Means of the signal values for each 30 seconds long task period is calculated. There were two task periods for each applied stimulus frequency. The mean of the two task periods that belonged to the same stimulus frequency is calculated. After all, for each stimulation frequency, the mean of the 13 subjects' task periods were calculated.

6. RESULTS

6.1 Results of the EEG Data Analysis

The average EEG responses of the two central frontal electrodes were calculated (AFz and Fz) and compared with the central occipital electrode Oz in order to investigate the ssVEP power differences of the two regions and the differences in their responses to varying stimulation frequencies. The mean of the EEG responses of 13 subjects were calculated.

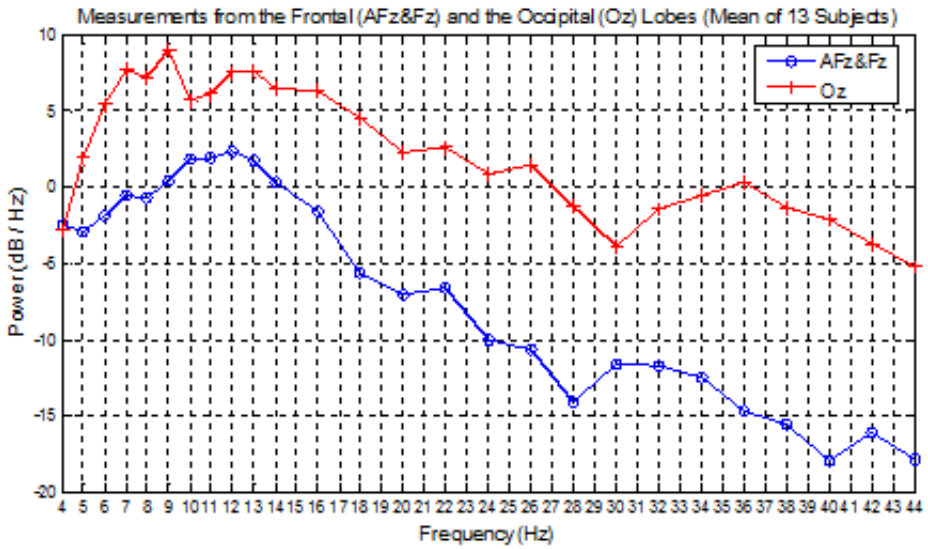

Figure 6.1 ssVEP powers of 13 subjects obtained from the central frontal and central occipital regions

The amplitude of the EEG response that was obtained from the occipital electrode is greater than the response of the EEG amplitude recorded from the frontal electrodes. However the response recorded from both regions display a similar trend with respect to stimulation frequency. One -way ANOVA analysis was performed in a frequency-by-frequency manner on the frontal and occipital responses and at 4, 10, 11 and 12 Hz visual stimulation, ssVEP powers of the frontal and the occipital regions are not significantly different ($p>0.05$). The same analysis was also performed on the normalized frontal and occipital responses and at 4, 8, 9, 10, 11, 12, 13 and 14 Hz

visual stimulation, ssVEP powers of the frontal and the occipital regions also turned out to be similar ($p>0.05$). The maximal ssVEP power is observed at 9 Hz for the occipital region. The ssVEP power peaks at 10-13 Hz (upper alpha band) stimulation frequencies for the frontal region. At 4 Hz stimulation frequency the frontal and the occipital ssVEP powers are the same. The ssVEP power of both the frontal and the occipital regions are minimal for 44 Hz stimulation frequency.

Powers of the ssVEPs recorded from the left hemisphere and the right hemisphere were also compared with each other. ssVEP power obtained from the left frontal electrodes (F3&F7) was compared with the ssVEP power obtained from the right frontal electrodes (F4&F8). In the same manner the ssVEP power obtained from the left occipital electrode (O1) was compared with the ssVEP power obtained from the right occipital electrode (O2).

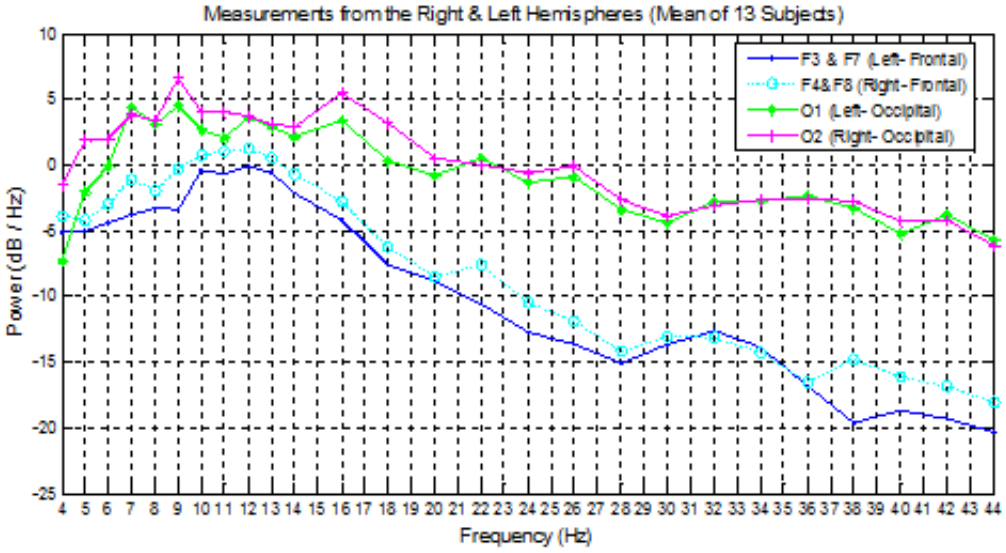

Figure 6.2 Mean ssVEP powers of 13 subjects obtained from the right and left frontal and occipital regions

The EEG response recorded from both the right and left hemisphere electrodes significantly differed for varying stimulation frequencies due to the one-way ANOVA test ($p=0$). One way ANOVA test revealed no significant differences between the frontal right and frontal left electrodes. Occipital right and occipital left electrodes also display no significant differences except for the 4 and 5 Hz stimulation frequencies.

The mean of the frontal electrodes was calculated by averaging the F3, F4, F7, F8, Fz and AFz records and the mean of the occipital electrodes was calculated by averaging O1, O2 and Oz records in order to obtain the distributed frontal and occipital electrophysiological response.

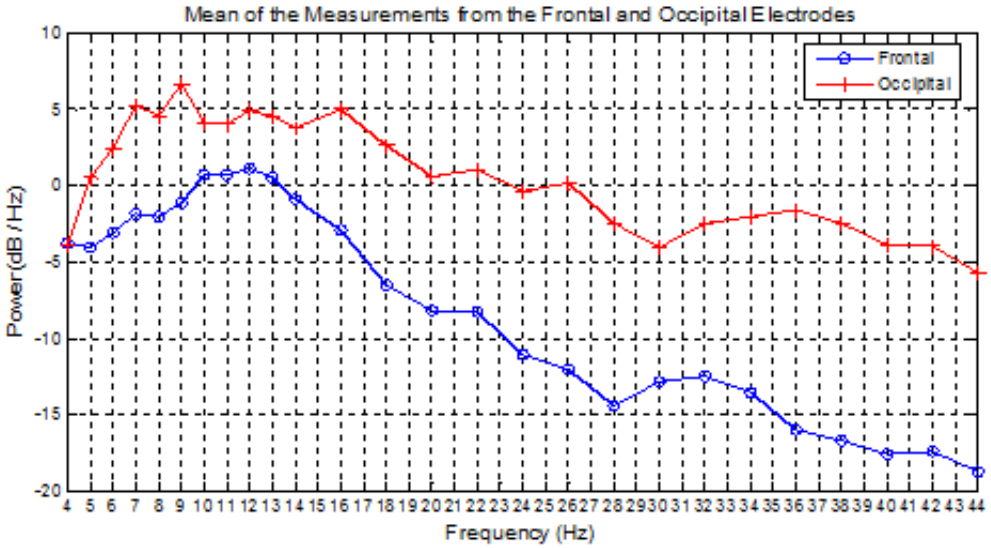

Figure 6.3 Mean ssVEP powers of 13 subjects obtained from the entire frontal and occipital regions

The maximum occipital ssVEP power is observed at 9 Hz whereas the maximum frontal ssVEP power is observed at 12 Hz. Secondary peaks are observed at 7, 12 and 16 Hz and a broad peak is observed between 32-38 Hz stimulation frequencies for the occipital region. For the frontal region the ssVEP power peaks in the 10-13 Hz (upper alpha band) region and a broad peak is observed in the 30-34 Hz stimulation frequency range. The amplitudes of the ssVEP powers from both regions decreased with the increasing stimulation frequencies and the minimum responses were observed at 44 Hz. At 4 Hz stimulation frequency the ssVEP powers of both regions were the same.

6.2 Results of the fNIRS Data Analysis

The mean HBO2 signal that was obtained from the 3rd and the 7th detectors of the fNIRS probe during stimulation periods is averaged between 13 subjects. The

3rd detector corresponded to the left hemisphere and the 7th detector corresponded to the right hemisphere.

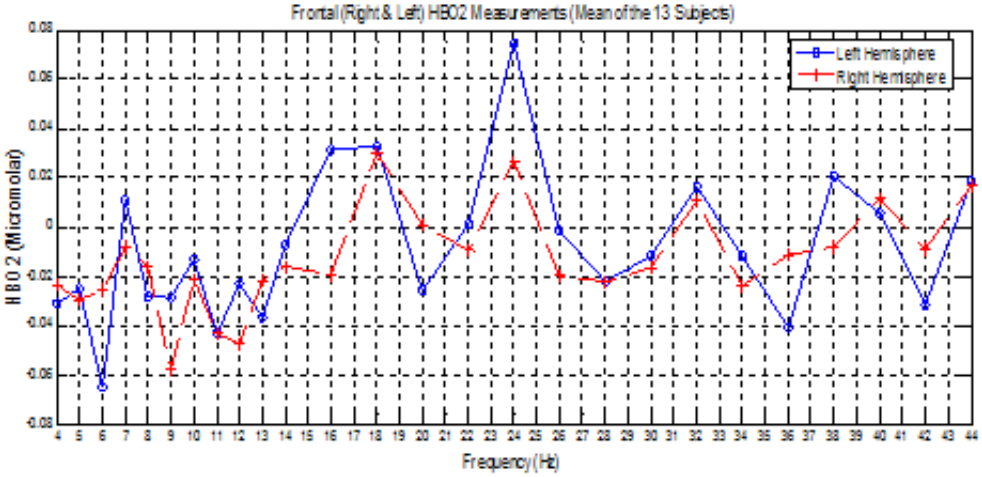

Figure 6.4 Mean HBO2 values from the right and the left hemispheres of 13 subjects

In the one-way ANOVA test no significant differences between the HBO2 responses of the right and left hemispheres were found. Therefore mean of the 3rd and 7th detectors were used for the rest of the analysis.

One way ANOVA test was performed between groups consisting of three adjacent stimulation frequencies. Although right and left hemispheres do not differ significantly in terms of HBO2 response, only in the one-way ANOVA test of the left hemisphere, 20-22-24 Hz and 22-24-26 Hz groups were found to display significant differences ($p<0.05$).

In order to display the distribution of the hemodynamic response on the frontal cortex, the mean of the 3rd (left hemisphere) and the 7th (right hemisphere) channel was calculated.

The maximum HBO2 response was observed at 24 Hz, and a secondary peak was observed at 18 Hz stimulation frequency. Local peaks were observed at 7, 10, 32 and 40 Hz stimulation frequencies.

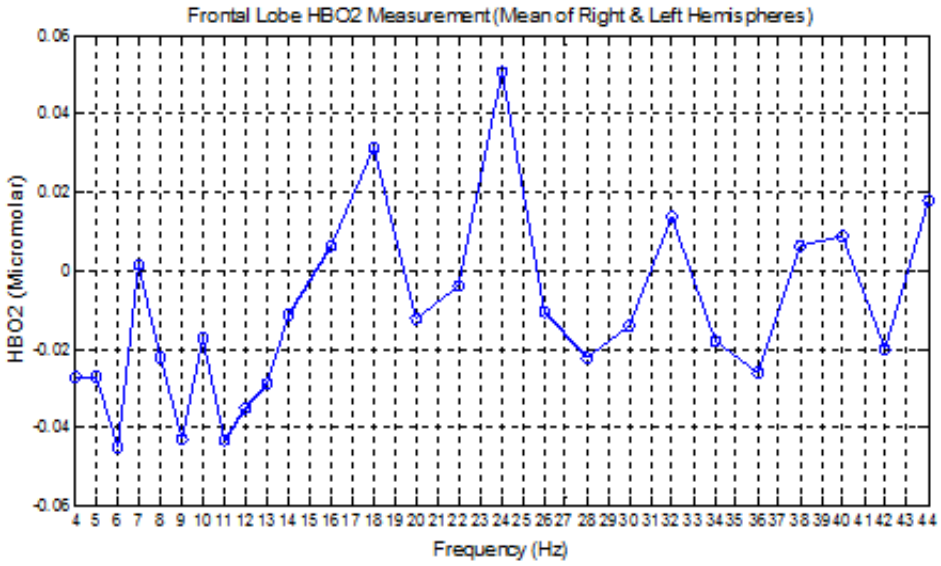

Figure 6.5 Mean of the right and the left hemispheres

6.3 EEG-fNIRS Correlation

The correlation of the hemodynamic response to the electrophysiological response is calculated for all stimulation frequencies. At 9, 12, 20, 28 and 30 Hz the probability values were smaller than 0.05. The ssVEP and HBO2 responses are positively correlated ($0.5 < r < 0.7$) for 9, 12 and 20 Hz and negatively correlated ($-0.07 < r < -0.5$) for 28 and 30 Hz stimulation frequencies. A strong hemodynamic response was observed at 24 Hz. We assumed that this may indicate a neurovascular coupling at that stimulation frequency. However the correlation of the hemodynamic response to the electrophysiological response at 24 Hz turned out to be weak.

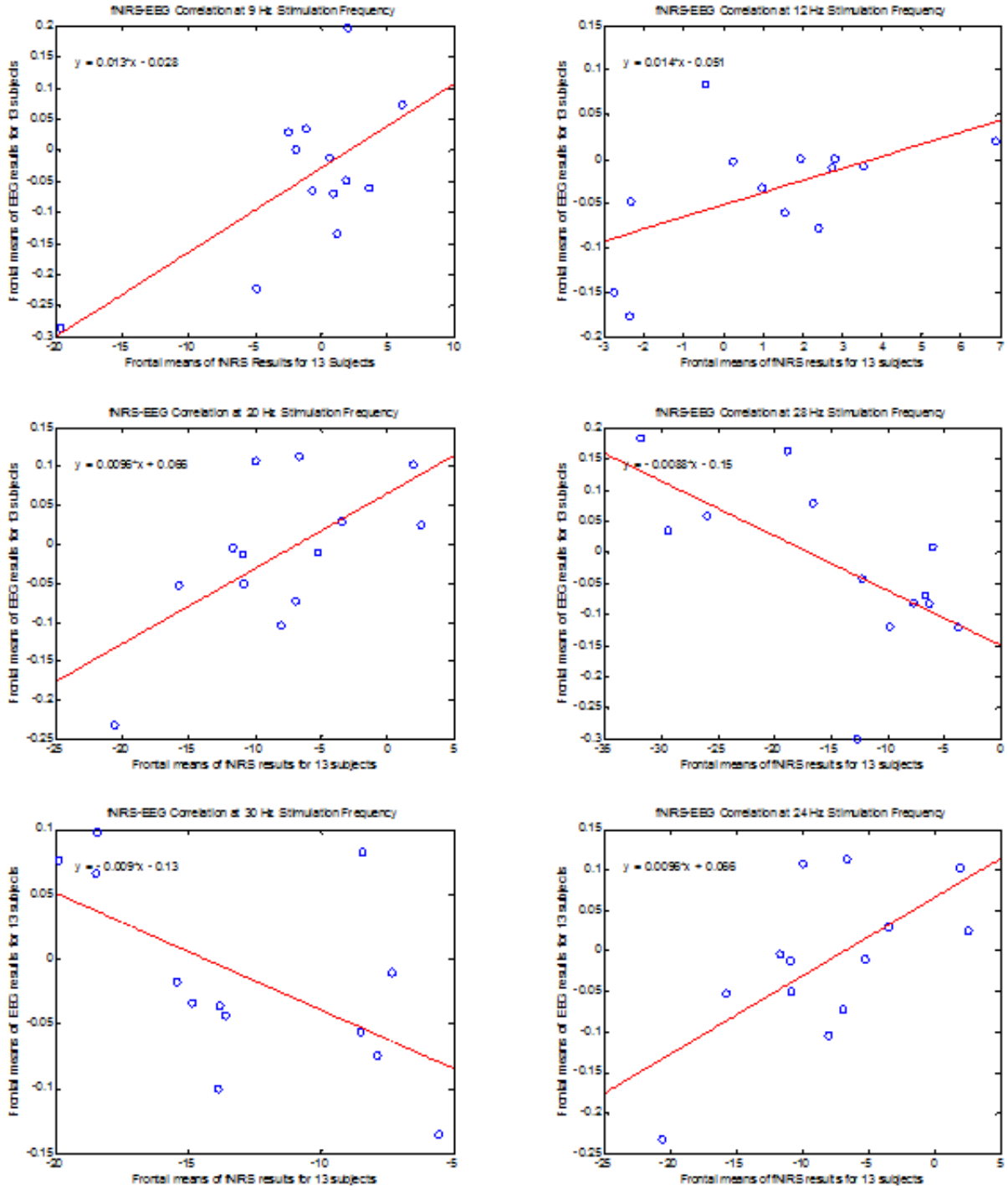

Figure 6.6 Correlation between the ssVEP and hemodynamic responses of the frontal lobes of 13 subjects at a) 9, b) 12, c) 20, d) 28, e) 30 and f) 24 Hz stimulation

7. DISCUSSION

Different neuroimaging models monitor different aspects of the vascular response modality, all of which are sequels of the disproportionally large increase in CBF [18]. Obrig et al. showed that optical methods are able to directly demonstrate the focal hyper-oxygenation in response to a stimulus, when measuring over the corresponding optical area [28]. The potential of NIRS to detect changes in cerebral oxygenation in response to functional stimulation has been demonstrated in previous studies [27, 29]. Functional near infrared spectroscopy (fNIRS) has been used in various studies in order to investigate the regulation of the hemodynamic response to functional stimulation. Boden et al. investigated the lag between the fNIRS parameters (oxy-Hb and deoxy-Hb) in response to an alternating hand motor paradigm [18].

Combined imaging modalities allow the simultaneous monitoring of the brain's hemodynamic and electrophysiological activity in response to sensory stimulation. fNIRS can be used simultaneously with other imaging techniques as has been shown in earlier studies. In a simultaneous EEG and fNIRS study Koch et al. investigated the correlation of the resting state individual alpha frequency with the amplitudes of neuronal and vascular responses to visual stimulation [30]. In another simultaneous EEG and fNIRS study Koch et al. exposed the subjects to flicker frequencies varying from 1 to 25 Hz and investigated the modulations of alpha power and its correlations with the VEP and vascular responses [31]. Moosmann et al. investigated the correlations of the occipital EEG alpha rhythm changes with changes in local cerebral blood oxygenation by using simultaneous EEG-fMRI and EEG-fNIRS measurements [32].

Functional brain networks that process sensory inputs can be investigated using steady-state paradigms that impose synchrony on populations of cortical neurons with a periodic stimulus [2]. In EEG recordings in humans, a few hundred milliseconds after the onset of repetitive visual stimulation, steady-state visual-evoked response (ssVER) appears in the occipital leads [33, 34]. Occipital ssVEPs can be recorded at

most flicker frequencies. In contrast, ssVEPs are recorded over parietal, temporal, and frontal lobes over narrow frequency range [2, 3, 4, 6, 35, 36]. Srinivasan et al. presented their subjects random dot patterns flickering with frequencies varying from 3 to 30 Hz and recorded their EEG [36]. They observed the maximum responses at occipital and parietal electrodes for flicker frequencies within delta (f=3 Hz), lower alpha (f=8 Hz) and upper alpha (f=12 and 13 Hz) bands. They also observed responses at most flicker frequencies with lower magnitudes (by a factor of 2) at frontal electrodes than occipital and parietal. They observed the strongest frontal responses for flicker frequencies in the delta (f = 3 Hz), lower alpha (f = 7 and 8 Hz) and upper alpha (f= 12 and 13 Hz) bands. They found out that the spatial distribution of the frontal ssVEP power depends on the flicker frequency and that the frontal ssVEPs are concentrated over midline electrodes in the delta and lower alpha bands while lateral areas show stronger ssVEPs in the upper alpha band. They observed that at f = 7 Hz, ssVEP power is higher over the left hemisphere, while at f = 13 Hz, ssVEP power is higher over the right hemisphere.

In a simultaneous EEG and PET study, Pastor et al. presented the subjects flash frequencies of 5, 10, 12, 15, 17, 20, 22, 25, 27, 30, 35, 40, 47 and 60 Hz [34]. They observed that the oscillatory response reached the greatest amplitude at 15 Hz in the occipital area and at 25 Hz in frontal areas and subsequently decreased at higher click rates. However in PET recording, the maximal rCFB response was obtained at 8 Hz, declining in amplitude at higher frequencies [37, 38]. Emir et al. investigated the dependency of positive BOLD signal of he temporal frequency of visual stimulation varying between 1 and 44 Hz [39]. They observed that the positive BOLD signal peaked at 8 Hz in primary visual cortex and secondary peaks were observed at 16 and 24 Hz. They also observed a broader peak around 36-40 Hz. Similarly Parkes et al. tried the 4-20 Hz stimulation frequencies in their fMRI study and reported that positive BOLD signal peaked at 8 Hz and reached a plateau for the stimulation frequencies above 8 Hz for the occipital voxels [40]. Singh et al. acquired EEG and BOLD fMRI data from the occipital region during stimulation at frequencies ranging from 2 to 12 Hz and observed that both the EEG and BOLD signals peak at approximately 8 Hz [41].

This study was a pioneering work because it compares the VEP response of the frontal cortex to that of the occipital cortex. Occipital lobe is the part of the brain that is associated with visual perception; therefore the most powerful response to visual stimulation is expected to appear at the occipital electrodes. In this study we assumed that the response of the brain to visual stimulation will be detectable throughout the brain and focused on the projection of the ssVEP on the frontal cortex. Another innovative aspect of this study is the comparison of the electrophysiological response of the frontal cortex to the hemodynamic response of the frontal cortex.

The fNIRS measurements from the frontal cortex revealed that the HBO2 signal was observed at the 24 Hz stimulation frequency. Secondary peaks were observed at 8, 10, 18, 32 Hz and a broader peak was observed between 38-40 Hz stimulation frequencies. The strongest hemodynamic response of the occipital cortex to visual stimulation is observed at 8 Hz stimulation frequency in earlier studies. However in our study, frontal cortex's hemodynamic response at 8 Hz stimulation frequency is observed to be comparatively weak. The ANOVA test comparing the adjacent frequencies revealed that there is significant HBO2 signal change ($p<0.05$) at the left frontal region between 6 and 7 Hz stimulation frequencies. The maximal peak at 24 Hz and the secondary peak observed at 18 Hz exhibit similarities with the findings of Emir et al. in which local maximums were observed at 24 and 16 Hz [39]. The broad peak observed at 38-40 Hz is also consistent with the broad peak Emir et al. observed 36-40 Hz [39]. The ANOVA test performed on adjacent frequencies two at a time revealed that the HBO2 response of the left frontal region to stimulation frequencies between 22-24 and 24-26 Hz differ significantly ($p<0.05$).

EEG records from the occipital electrodes revealed that the VEP power is maximal for the 9 Hz stimulation frequency and secondary peaks occur at 7, 12 and 16 Hz. Between 16 Hz and 30 Hz stimulation frequencies the VEP power decreases but local peaks occur at 22 and 26 Hz and finally a broad peak is observed between 30-40 Hz. Srinivasan et al. observed the maximum ssVEP response at 3, 8, 12 and 13 Hz stimulation frequencies [36] and Pastor et al. observed maximum ssVEP response at 15 Hz [34]. The findings of this study exhibit similarities with the findings of these former

studies as the VEP power peaks observed in this study also fall into the lower alpha (8-10 Hz) and upper alpha (10-13 Hz) bands. The peak observed at 16 Hz falls into the lower beta band as the peak Pastor et al. observed at 15 Hz stimulation frequency [36]. Maximum ssVEP power obtained from the frontal electrodes is observed in the upper alpha band (10-13 Hz). Srinivasan et al. also observed an ssVEP peak at 12-13 Hz stimulation frequency which also falls into the upper alpha frequency band [36]. A decrease in the ssVEP power is observed between 12-28 Hz stimulation frequencies including a local peak at 22Hz. A local peak is also observed at 7 Hz and a broad peak is observed between 28-36 Hz stimulation frequencies. The peaks observed at 12 Hz, 7 Hz and 22 Hz are common for both the frontal and the occipital regions. The response of the frontal and the occipital regions to 4 Hz stimulation frequency in terms of ssVEP power is observed to be the same. The minimum ssVEP power obtained from both regions is observed at 44 Hz stimulation frequency. ANOVA tests are performed over the whole stimulation frequency range for both the occipital and the frontal records and the test results turned out to be significantly different ($p=0$).

In this study we intend to put forward the common stimulation frequencies that both the electrophysiological and the hemodynamic responses of the frontal lobe of the human brain favor the most. To do so we analyzed the correlation of the ssVEP responses that were obtained from the frontal regions of 13 subjects at a certain stimulation frequency with the HBO2 measurements that were obtained from the frontal regions of the subjects at the same stimulation frequency. We repeated the same correlation analysis for each 26 stimulation frequencies and observed that at 9, 12, 20, 28 and 30 Hz the probability values were smaller than 0.05 and the correlation coefficient values imply a moderate linear relationship. The ssVEP and HBO2 responses are positively correlated ($0.5< r <0.7$) for 9, 12 and 20 Hz and negatively correlated ($-0.7< r <-0.5$) for 28 and 30 Hz stimulation frequencies.

At 12 Hz the power of the ssVEP response of the frontal lobe was maximal; additionally ssVEP and hemodynamic responses are found to be moderately correlated at 12 Hz. These findings tempt us to assume that 12 Hz visual stimulation lead to a strong neurovascular coupling. As the strongest hemodynamic response was observed

at 24 Hz stimulation frequency, we supposed that 24 Hz may also cause a strong neurovascular coupling; however the correlation of the ssVEP and hemodynamic responses at that stimulation frequency turned out to be weak.

8. CONCLUSION

We investigated the effects of repetitive visual stimulation at various stimulation frequencies on the neural activity and cerebral oxygenation. To do so we explored a wide range of stimulation frequencies consisting of 26 distinct frequencies. We focused on the power of the ssVEP signal elicited at the occipital and frontal cortecies and the HBO2 concentration changes that occur at the frontal cortex.

The results of this study suggest that the ssVEP responses of the frontal and the occipital cortecies follow a similar trend with respect to stimulation frequency although the power of the ssVEPs elicited at the occipital cortex is much higher. The maximal ssVEP power was obtained from the occipital cortex at 9 Hz and from the frontal cortex at 12 Hz. The maximal hemodynamic response of the frontal cortex was observed at 24 Hz stimulation frequency. As we compared the electrical activity of the frontal cortex to its hemodynamic response, we found a positive linear correlation at 9, 12 and 20 Hz stimulation frequencies and a negative linear correlation at 28 and 30 Hz stimulation frequencies.

We investigated a broad range of stimulation frequencies on 13 subjects in this study. In order to further confirm our results we have to apply the same paradigm on more subjects. In our EEG analysis we used stimulus- locked signal averaging method in order to extract the ERPs from the spontaneous EEG activity. To further increase the signal-to-noise ratios of our records and to eliminate the trial-to-trial variability in latency problem, we may have also tried other signal averaging methods. We may also search for the sources of the neural activity by applying source localization algorithms. In our fNIRs analysis, we calculated the mean values of the HBO2 signal amplitudes recorded during the stimulation periods. As a future plan we may try mathematical algorithms such as Independent Component Analysis (ICA) or statistical methods like General Linear Models (GLM) to investigate the cerebral oxygenation.

REFERENCES

1. Regan, D., "Some characteristics of average steady-state and transient responses evoked by modulated light," *Electroencephalogy and Clinical Neurophysiology*, Vol. 20, pp. 238–248, 1966.

2. Srinivasan, R., E. Fornari, M. G. Knyazeva, R. Meuli, and P. Maeder, "fmri responses in medial frontal cortex that depend on temporal frequency of visual input," *Exp Brain Res.*, Vol. 180, pp. 677–691, 2007.

3. Srinivasan, R., D. P. Russell, G. M. Edelman, and G. Tononi, "Increased synchronization of neuromagnetic responses during conscious perception," *J Neurosci*, Vol. 19, pp. 5435–5448, 1999.

4. Srinivasan, R., "Internal and external nueral synchronization during conscious perception," *Int J Bifurcat Chaos*, Vol. 19, pp. 1–18, 2004.

5. Srinivasan, R., and S. Petrovic, "Meg phase follows conscious perception during binocular rivalry induced by visual stream segregation," *Cereb Cortex*, Vol. 16, pp. 597–608, 2006.

6. Ding, J., G. Sperling, and R. Srinivasan, "Attentional modulation of ssvep power depends on the network tagged by the flicker frequency," *Cerebral Cortex*, Vol. 16, pp. 1016–1029, 2006.

7. Chen, Y., and A. K. S. J. A. G. G. M. Edelman, "The power of human brain magnetoencephalographic signals can be modulated up or down by changes in an attentive visual task," *Proc Natl Acad Sci USA*, Vol. 100, pp. 3501–3506, 2003.

8. Silberstein, R. B., P. L. Nunez, A. Pipingas, P. Harris, and F. Danieli, "Steady state visually evoked potential (ssvep) topography in a graded working memory task," *Int J Psychophysiol*, Vol. 42, pp. 219–232, 2001.

9. "Neuron." Available: http://www.webbooks.com/eLibrary/Medicine/Physiology/Nervous/neuron.jpg.

10. "Parts of the brain." Available: http://www.medindia.net/patients/patientinfo/Images/Brain_parts.gif.

11. "Lobes of the brain." Available: http://www.shands.org/health/graphics/images/en/9549.jpg.

12. "Hemoglobin molecule." Available: http://images.absoluteastronomy.com/images/ encyclopediaimages/h/he/heme.svg.png.

13. "Astrocyte-neuron lactate shuttle." Available: http://neurology4medics.com/Glial_Figure_2.gif.

14. Roy, C., and C. Sherrington, "On the regulation of the blood supply of the brain," *J. Physiol*, Vol. 11, pp. 85–108, 1890.

15. Attwell, D., and C. Iadecola, "The neural basis of functional brain imaging signals," *Trends Neurosci*, Vol. 25, pp. 621–625, 2002.

16. Lauritzen, M., "Reading vascular changes in brain imaging: is dendritic calcium the key?," *Nature reviews*, Vol. 6, pp. 77–85, 2005.

17. Fox, P. T., and M. E. Raichle, "Focal physiological uncoupling of cerebral blood flow and oxidative metabolism during somatosensory stimulation in human subjects," *Proc. Natl. Acad. Sci. USA*, Vol. 83, pp. 1140–1144, 1986.

18. Boden, S., H. Obrig, C. Köhncke, H. Benav, S. P. Koch, and J. Steinbrink, "The oxygenation response to functional stimulation: is there a physiological meaning to the lag between parameters?," *NeuroImage*, Vol. 36, pp. 100–107, 2007.

19. "Neurovascular coupling." Available: http://www.scholarpedia.org/wiki/images/9/9f/PasleyNV3.jpg.

20. Luck, S. J., *An Introduction to the Event-Related Potential Technique*, Cambridge Massachusetts: THE MIT PRESS, 2005. Available: http://mitpress.mit.edu.

21. Collura, T. F., "Human steady-state visual and auditory evoked potential components during a selective discrimination task," *Journal of Neurotheraphy*, Vol. 1, no. 3, pp. 1–9, 1995.

22. Jöbsis, F. F., "Noninvasive, infrared monitoring of cerebral and myocardial oxygen suficiency and circulatory parameters," *Science*, Vol. 198, pp. 1264–1267, 1977.

23. Young, A. E. R., T. J. Germon, N. J. Barnett, A. R. Manara, and R. J. Nelson, "Behavior of near-infrared light in the human health: implications for clinical near-infrared spectroscopy," *British Journal of Anaesthesia*, Vol. 84, no. 1, pp. 38–42, 2000.

24. "Absorption spectra of chromophores." Available: http://www.rsc.org/ej/PP/2003/b209651j-f2.gif.

25. Boas, D. A., M. A. Franceschini, a K Dunn, and G. Strangman, "Noninvasive imaging of cerebral activation with diffuse optical tomography," *In Vivo Optical Imaging of Brain Function*, pp. 193–221, 2002.

26. Bozkurt, A., A. Rosen, H. Rosen, and B. Onaral, "A portable near infrared spectroscopy system for bedside monitoring of newborn brain," *BioMedical Engineering OnLine*, pp. 4–29, 2005.

27. Villringer, A., and B. Chance, "Non-invasive optical spectroscopy and imaging of human brain function," *Trends in Neurosciences*, Vol. 20, no. 10, pp. 435–442, 1997.

28. Obrig, H., R. Wenzel, M. Kohl, S. Horst, P. Wobst, J. Steinbrink, F. Thomas, and A. Vilringer, "Near-infrared spectroscopy: does it function in functional activation studies of the adult brain?," *Int. J. Psychophysiol.*, Vol. 35, pp. 125–142, 2000.

29. Obrig, H., C. Hirth, J. G. Junge-Hulsing, C. Doge, T. Wolf, U. Dirnagl, and A. Villringer, "Cerebral oxygenation changes in response to motor stimulation," *J. Appl. Physiol.*, Vol. 81, pp. 1174–1183, 1996.

30. Koch, S. P., S. Koedgen, R. Bourayou, J. Steinbrink, and H. Obrig, "Individuall alpha-frequency correlates with amplitude of visual evoked potential and hemodynamic response," *NeuroImage*, Vol. 41, pp. 233–242, 2008.

31. Koch, S. P., S. Steinbrink, A. Villringer, and H. Obrig, "Synchronization between background activity and visually evoked potentials is not mirrored by hyperoxygenation: implications fot the interpretation of vascular brain imaging," *The Journal of Neuroscience*, Vol. 26, no. 18, pp. 4940–4048, 2006.

32. Moosmann, M., P. Ritter, I. Krastel, A. Brink, S. Thees, F. Blankenburg, B. Taksin, H. Obrig, and A. Villringer, "Correlates of alpha rhythm in functional magnetic resonance imaging and near infrared spectroscopy," *Neuroimage*, Vol. 20, pp. 145–158, 2003.

33. Regan, D., "An effect of stimulus color on average steady-state potentals evoed in man," *Nature*, Vol. 210, pp. 1056–1057, 1966.

34. Pastor, M. A., J. Artieda, J. Arbizu, M. Valencia, and J. c Masdeu, "Human cerebral activation during steady state visual evoked responses," *The Journal of Neuroscience*, Vol. 23, no. 37, pp. 11621–11627, 2003.

35. Narici, L., K. Portin, R. Salmelin, and R. Hari, "Responsiveness of human cortical activity to rhythmical stimulation: a three modality whole cortex neuromagnetic investigation," *NeuroImage*, Vol. 7, pp. 209–223, 1998.

36. Srinivasan, R., F. A. Bibi, and P. L. Nunez, "Steady-state visual evoked potentials: distributed local sources and wave-like dynamics are sensitive to flicker frequency," *Brain Topogr.*, Vol. 18, no. 3, pp. 167–187, 2006.

37. Fox, P. T., and M. E. Raichle, "Stimulus rate determines regional brain blood flow in striate cortex," *Ann NeuroI*, Vol. 17, pp. 303–305, 1985.

38. Mentis, M. J., G. E. Alexander, C. L. Grady, B. Horwitz, J. Krasuski, P. Pietrini, T. Strassburger, H. Hampel, M. B. Schapiro, and S. I. Rapoport, "Frequency variation of a pattern-flash visual stimulus during pet differentially activates brain from striate through frontal cortex," *NeuroImage*, Vol. 5, pp. 116–128, 1997.

39. Emir, U. E., Z. Bayraktaroğlu, C. Öztürk, A. Ademoğlu, and T. Demiralp, "Changes in bold transients visual stimuli across 1-44 hz," *Neuroscience Letters*, Vol. 436, pp. 185–188, 2008.

40. Parkes, L. M., P. Fries, C. M. Kerskens, and D. G. Norris, "Reduced bold response to periodic visual stimulation," *Neuroimage*, Vol. 21, pp. 236–243, 2004.

41. Singh, M., S. Kim, and T. Kim, "Correlation between bold-fmri and eeg signal changes in response to visual stimulus frequency in humans," *Magnetic Resonance in Medicine*, Vol. 49, pp. 108–114, 2003.